Local biodiversity change reflects interactions among changing abundance, evenness and richness

Shane A. Blowes, German Centre for Integrative Biodiversity Research (iDiv) Halle-Jena-Leipzig, Germany; Department of Computer Science, Martin Luther University Halle-Wittenberg, Halle (Salle), Germany. shane.blowes@idiv.de

Gergana N. Daskalova, School of GeoSciences, University of Edinburgh, Scotland EH9 3FF. gndaskalova@gmail.com

Maria Dornelas, Centre for Biological Diversity, University of St Andrews, KY16 9TH. maadd@st-andrews.ac.uk

Thore Engel, German Centre for Integrative Biodiversity Research (iDiv) Halle-Jena-Leipzig, Germany; Department of Computer Science, Martin Luther University Halle-Wittenberg, Halle (Salle), Germany. thore.engel@idiv.de

Nicholas J. Gotelli, Department of Biology, University of Vermont, Burlington, VT 05405 USA. Nicholas.Gotelli@uvm.edu

Anne E. Magurran, Centre for Biological Diversity, University of St Andrews, KY16 9TH. aem1@st-andrews.ac.uk

Inês S. Martins, Leverhulme Centre for Anthropocene Biodiversity and Department of Biology, University of York, York YO10 5DD, UK; Centre for Biological Diversity, University of St Andrews, KY16 9TH. iism1@st-andrews.ac.uk

Brian McGill, School of Biology and Ecology and Mitchell Center for Sustainability Solutions, University of Maine; Orono, ME. mail@brianmcgill.org

Daniel J. McGlinn, Department of Biology, College of Charleston, Charleston, SC. danmcglinn@gmail.com

Alban Sagouis, German Centre for Integrative Biodiversity Research (iDiv) Halle-Jena-Leipzig, Germany; Department of Computer Science, Martin Luther University Halle-Wittenberg, Halle (Salle), Germany. alban.sagouis@idiv.de

Hideyasu Shimadzu, Department of Mathematical Sciences, Loughborough University, LE11 3TU, UK; Graduate School of Public Health, Teikyo University, Tokyo, Japan. H.Shimadzu@lboro.ac.uk

Sarah R. Supp, Data Analytics Program, Denison University, Granville, OH 43023 USA. supps@denison.edu

Jonathan M. Chase, German Centre for Integrative Biodiversity Research (iDiv) Halle-Jena-Leipzig, Germany; Department of Computer Science, Martin Luther University Halle-Wittenberg, Halle (Salle), Germany. jonathan.chase@idiv.de

Running title: Characterizing multicomponent diversity change

Corresponding author: Shane Blowes, German Centre for Integrative Biodiversity Research (iDiv) Halle-Jena-Leipzig, Deutscher Platz 5e, Leipzig 04103, Germany. shane.blowes@idiv.de +49 341 9733254.

Open research statement: All data used in the manuscript are already in the public domain. The BioTIME database is accessible through the BioTIME website (http://biotime.st-andrews.ac.uk) and a Zenodo repository (https://zenodo.org/record/1095627). Perturbed time series were compiled using the data portal of the Environmental Data Initiative (https://portal.edirepository.org/nis/home.jsp), query as described in the methods; code for compilation and standardization available at https://github.com/chase-lab/BioTIMEx; upon acceptance, this code will be stored in combination with the code for analyses (see below) in Zenodo. The 2016 release of the PREDICTS database as used here is available at https://data.nhm.ac.uk/dataset/the-2016-release-of-the-predicts-database. McGill SAD data were previously archived at: https://doi.org/10.6084/m9.figshare.6945704. CESTES database is available at https://doi.org/10.25829/idiv.286-21-2695. Code for all analyses is available at https://github.com/sablowes/MulticomponentBioChange; upon acceptance, this code will be stored (with code for accessing and cleaning the EDI data described above) in Zenodo.

Abstract

Biodiversity metrics often integrate data on the presence and abundance of multiple species. Yet understanding covariation of changes to the numbers of individuals, the evenness of species' relative abundances, and the total number of species remains limited. Using individual-based rarefaction curves, we introduce a conceptual framework to understand how expected positive relationships among changes in abundance, evenness and richness arise, and how they can break down. We then examined interdependencies between changes in abundance, evenness and richness in more than 1100 assemblages sampled either through time or across space. As predicted, richness changes were greatest when abundance and evenness changed in the same direction, and countervailing changes in abundance and evenness acted to constrain the magnitude of changes in species richness. Site-to-site changes in abundance, evenness, and richness were often decoupled, and pairwise relationships between changes in these components across assemblages were weak. In contrast, changes in species richness and relative abundance were strongly correlated for assemblages varying through time. Temporal changes in local biodiversity showed greater inertia and stronger relationships between the component changes when compared to site-to-site variation. Local variation in assemblage diversity was rarely due to a passive sample from a more or less static species abundance distribution. Instead, changing species relative abundances often dominated local variation in diversity. Moreover, how changing relative abundances combined with changes to total abundance frequently determined the magnitude of richness changes. Embracing the interdependencies between changing abundance, evenness and richness can provide new information for better understanding biodiversity change in the Anthropocene.

Keywords: biodiversity change, abundance, evenness, species richness, rarefaction

Introduction

Measures of biodiversity and its change are frequently used to determine the magnitude, direction and pace of ecosystem modifications (Diaz et al. 2019). Descriptions of the distribution and abundance of organisms are central to basic ecological research (Krebs 1972, Andrewartha & Birch 1984), and biodiversity (as applied to taxonomic or species diversity) is a multifaceted concept that combines information on the distribution and abundance of multiple species. There have been numerous such aggregate metrics proposed to quantify different aspects of biodiversity (e.g., Hill 1973, Gotelli and Colwell 2001, Magurran & McGill 2011, Chao and Jost 2012), most of which depend on sample effort and scale (Rosenzweig 1995, Whittaker et al. 2001, McGill 2011a, Chase & Knight 2013). This inherent complexity poses significant challenges for quantitative syntheses of temporal and spatial variation in biodiversity.

Here, we argue that in order to understand biodiversity change, it is critical to look beyond aggregate metrics in isolation. Specifically, we need to examine how changes in the key components that lead to aggregate metrics interact and combine with each other. Currently, different components that underlie biodiversity represent important, but are largely viewed as independent lines of evidence for contemporary biodiversity change. For example, one body of work is focused on quantifying total abundances of all species within assemblages, such as recent work documenting declines of birds (e.g., Rosenberg et al. 2019) and insects (Wagner 2020). A related body of work focuses instead on population-level ‘winners’ and ‘losers’ within assemblages (McKinney & Lockwood 2000), species with increasing and decreasing trends in occupancy or abundance (e.g., WWF 2020). However, changes in the means of these metrics do not capture the variability and nuance in either the assemblage- and population-level abundance

trends across space and among taxa (e.g., van Klink et al. 2020, Daskalova et al. 2020a, Leung et al. 2020). Moreover, trends in total assemblage abundance provide only one window into potentially complex changes that could be occurring in other components of biodiversity, and while changes to species relative abundances do influence biodiversity metrics, population-level trends themselves cannot be used to calculate assemblage-level (i.e., biodiversity) metrics (e.g., Dornelas et al. 2019). Even when quantifying the same response metric (i.e., species richness), syntheses of biodiversity change in space due to differential land use conditions have found declines of species richness (e.g., Newbold et al. 2015, 2018), whereas analyses of time series have shown that, on average, species richness increases roughly offset decreases (Dornelas et al. 2014, Blowes et al. 2019), despite often significant modifications to climate and habitat (Antão et al. 2020a, Daskalova et al. 2020b). Finally, the prediction that human activities likely impact species relative abundances more frequently than species occurrences (Chapin et al. 2000), has not resulted in a strong focus on assemblage-level evenness in existing syntheses (but see, e.g., Crowder et al. 2010, Zhang et al. 2012, Jones & Magurran 2018). Importantly, changes in all these components -- abundance, evenness, and richness -- contribute to variation in biodiversity. Yet little is known about how components are changing in combination within assemblages, and whether certain combinations act to constrain observed biodiversity change.

Species origination (speciation plus colonization) and extinction are the most fundamental processes for biodiversity dynamics (Storch et al. 2021). These processes combine with productivity (Currie 1991, Mittelbach et al. 2001), disturbance frequency and intensity (Connell 1978, Miller et al. 2011), historical (Latham & Ricklefs 1993) and biogeographic factors (e.g., Kreft et al. 2008), land use modifications (Newbold et al. 2015), and climate change (Antão et al.

135 2020a) to drive variation in biodiversity. In turn, these processes and drivers combine such that
136 local scale measures of biodiversity estimated from a given (local) sample depends largely on
137 two components (see e.g., He and Legendre 2002, McGill 2011a). First, the total number of
138 individuals (Fisher et al. 1943, Preston 1962), whereby fewer individuals are expected to (non-
139 linearly) lead to fewer species. Second, the total number of species and their relative abundances
140 within the regional species pool (i.e., the set of all potential colonizing species in a region),
141 which we refer to as the Species Abundance Distribution (SAD; McGill et al. 2007). Local
142 samples will have lower species richness when the species pool has relatively few highly
143 abundant species and many rare species (i.e., less even SADs), compared to samples from a
144 species pool of the equivalent size with more equitable species abundances. Moreover, variation
145 or changes in local environmental conditions can alter local patterns of species relative
146 abundances. Whenever two or more samples across space or time differ in the total number of
147 individuals, the shape of the SAD, or both, there will be changes in most metrics of biodiversity.
148 However, changes in abundance and the SAD are not always correlated, and, when decoupled,
149 the magnitude and direction of change in derived biodiversity metrics can differ considerably.
150
151 Variation in the total number of individuals is a long-standing, first-order explanation of
152 variation in richness (Fisher et al. 1943, Coleman et al. 1982, Srivastava & Lawton 1998, Gaston
153 2000, Scheiner & Willig 2005, Storch et al. 2018). In the context of species-area relationships,
154 this has been termed the 'passive sampling hypothesis' (Coleman et al. 1982), and as local
155 assemblages increase in size they are expected to include more species from the regional pool
156 due to sampling processes alone. Larger (Connor & McCoy 1979) or more productive (Wright
157 1983) areas are also predicted to have more species driven again by increased numbers of

158 individuals, but in these cases associated with processes other than sampling, such as decreased
159 likelihood of species extinction with increased population sizes (Preston 1962, Wright 1983,
160 Srivastava & Lawton 1998), and commonly termed the 'more individuals hypothesis' (Srivastava
161 & Lawton 1998). Anthropogenic drivers can also influence the number of individuals in
162 assemblages (e.g., via eutrophication, exploitation, harvesting or land clearing), potentially
163 impacting biodiversity due to changes to the total number of individuals (Newbold et al. 2015,
164 Blowes et al. 2020). If biodiversity varies primarily via changes in the numbers of individuals,
165 positive relationships between altered numbers of individuals and species richness changes are
166 expected. In such cases, however, other metrics of species diversity that control for variation in
167 numbers of individuals, such as species richness expected for a given number of individuals—
168 known as rarefied richness—should be relatively unchanged.
169
170 Changes to the shape of the SAD can drive variation in biodiversity through time or space. For
171 example, co-occurrence and coexistence of species can be altered by changes to resource
172 diversity (MacArthur 1965), environmental or habitat heterogeneity (Tilman 1982, Shmida &
173 Wilson 1985), interspecific interactions (e.g., keystone predation; Paine 1974, Menge et al.
174 2020), biological invasions (Vilà et al. 2011), and external perturbations (Hughes et al. 2007).
175 Alterations to any of these features can change biodiversity by changing species' relative
176 abundances and the size of the species pool (via species additions or subtractions).
177 Anthropogenic factors can also favor some species and disfavor others, potentially altering the
178 relative abundance of species (e.g., due to selective exploitation; Blowes et al. 2020), or the size
179 of the species pool (e.g., species with large ranges replacing those with small ranges, Newbold et
180 al. 2018). In such cases, biodiversity change will be characterized by positive relationships

181 between species richness change and changes in metrics sensitive to relative abundance, such as
182 rarefied richness, evenness and diversity metrics sensitive to species relative abundances.
183
184 Changing components of biodiversity can covary in different and informative ways. Yet, to date,
185 there has been little exploration of this covariation in time or space, nor of the theoretical
186 linkages. For example, whether total abundances and the evenness of species' relative
187 abundances change in similar or decoupled ways, and how this influences biodiversity change is
188 largely unknown. However, syntheses of relationships between different biodiversity metrics,
189 which can reflect different combinations of component changes, have typically found
190 relationships to be weak. For example, Stirling and Wilsey (2001) showed that although strong
191 positive correlations between species richness, diversity and evenness metrics were expected
192 from a neutral model (Caswell 1976), there was considerable variation in the strength, and even
193 the sign of the relationships in 323 empirical comparisons. Similarly, Soininen et al. (2012)
194 examined temporal (n = 212) and spatial variation (n = 17) in aquatic datasets, and again found
195 considerable heterogeneity in the relationship between richness and evenness. Using data from
196 91 assemblages, McGill (2011b) concluded that most biodiversity metrics align with three axes
197 of empirical variation (total abundance, evenness and richness); components subsequently shown
198 to be relatively uncorrelated across space for a subset of 37 of the 91 assemblages (Chase et al.
199 2018). Collectively, these studies suggest that static biodiversity estimates are multidimensional,
200 and that different metrics can covary or be unrelated.
201
202 Where ecologists have quantified variation in multiple components of local diversity, the focus
203 has typically been on averages across assemblages, with each component treated as a separate,

independent response. For example, analyses of the local assemblages documented by the BioTIME database (Dornelas et al. 2018) show that numbers of individuals, species richness, and dominance (quantified as the relative abundance of the most numerically dominant species, and conceptually the complement of evenness) are highly variable among datasets, but on average, have no directional trend (Dornelas et al. 2014, Jones & Magurran 2018, Blowes et al. 2019). On the other hand, analyses of the PREDICTS database (Hudson et al. 2017) documenting spatial contrasts between assemblages in more pristine habitats with those in different land use categories, show that human-altered habitats frequently have fewer species and often fewer individuals (Newbold et al. 2015, 2020). However, these results describe average changes across assemblages estimated independently, whereas, as we describe in more detail below, component changes are unlikely to be completely independent.

Here, we first provide a conceptual overview of how changes in the main components underlying local biodiversity (total abundance, evenness and species richness) can combine using individual-based rarefaction curves. Using simplified scenarios with contrasting component changes, we show that the signs (or direction) of changes in total abundance and evenness can combine to determine the magnitude of expected richness changes, and whether positive pairwise relationships prevail. We then empirically assess interdependencies between abundance, evenness and richness changes using compilations of ecological assemblage data. In the face of natural and anthropogenically-driven environmental variation in time and space, we ask whether changes in the components of local biodiversity show positive relationships (i.e., change in the same direction). Or, alternatively, are component changes sufficiently heterogeneous that

226 variation in biodiversity depends on which of the underlying components (numbers of
227 individuals or the SAD) are changing, and how the different component changes combine?
228
229 **Conceptual relationships between changes in total abundance, evenness and richness**
230 Individual-Based Rarefaction (IBR) curves (Hurlbert 1971, Gotelli & Colwell 2001) are well
231 suited for visualizing conceptual relationships among changes in total abundance, evenness and
232 species richness (Fig. 1a, Cayuela et al. 2015, Chase et al. 2018, McGlinn et al. 2019). The end
233 point of the IBR depicts the total number of individuals of all species combined, and variation
234 between assemblages in where the IBR terminates quantifies changes to the number of
235 individuals (ΔN, Fig.1a) and species richness (ΔS, Fig. 1a). The shape (or curvature) of the IBR
236 curve reflects species' relative abundances and the size of the species pool (i.e., the SAD). We
237 use two parts of the curve to characterize changes in the SAD between assemblages. First,
238 because it is standardized to an equal number of individuals (n), changes in rarefied richness, ΔS_n
239 (Fig.1a), reflects changes to species' relative abundances only. Second, we use the numbers
240 equivalent (or effective number of species) transformation of the Probability of Interspecific
241 Encounter (PIE, Hurlbert 1971). The PIE is equal to the slope at the base of the rarefaction curve
242 (Olszewski 2004) and represents a metric of evenness that is relatively insensitive to sample
243 effort (more even communities have a higher PIE, Fig. 1a). Transformation of the PIE to the
244 numbers equivalent (S_{PIE}) aids comparisons to species richness (i.e., ΔS and ΔS_{PIE} have the same
245 units; Jost 2006). S_{PIE} is equal to the inverse of Simpson concentration (Jost 2006), and diversity
246 of order $q = 2$ (Hill 1973, Jost 2007), $D = (\sum_{i=1}^{S} p_i^q)^{1/(1-q)} = \frac{1}{\sum_{i=1}^{S} p_i^2}$, where S is the number of
247 species and p_i is the proportion of the assemblage represented by species i. As a consequence,

248 changes in S_{PIE} (ΔS_{PIE}) are most strongly influenced by the number of abundant or common
249 species in assemblages.
250
251 To visualize relationships among changes in total abundance, evenness and richness, we plot
252 pairwise relationships between changes in four components of the IBR. Specifically, changes in
253 species richness (ΔS) and total abundance (ΔN; Fig. 1b), and species richness and the two metrics
254 sensitive to changes in relative abundance – rarefied richness, ΔS_n (Fig. 1c), and ΔS_{PIE}, which we
255 refer to as evenness (Fig. 1d). Changing components with positive relationships (i.e., the same
256 sign) fall into the lower left and upper right quadrants, whereas assemblage changes that fall into
257 the upper left or lower right quadrants of Figs. 1b, c, d reflect a negative relationship between the
258 respective components.
259
260 Altered numbers of individuals, but no change to the SAD, can underpin differences in diversity
261 between assemblages. Changes only to the number of individuals being passively sampled from
262 the same underlying SAD (Fig. 2a) result in ΔS and ΔN being positively related with the same
263 sign (Fig. 2g), whereas ΔS_n (Fig. 2h) and ΔS_{PIE} (Figs. 2i) will be approximately zero (and have a
264 weak or no relationship with ΔS). This has been variously referred to in the literature as a
265 sampling effect, the rarefaction effect, and the passive sampling hypothesis (Coleman et al. 1982,
266 Gotelli & Cowell 2001, Palmer et al. 2000).
267
268 Changes in species richness (ΔS) can also be solely associated with changes to relative
269 abundance (i.e., $\Delta N \approx 0$), which weakens or removes the expectation for a positive relationship
270 between changes in richness and total abundance. For example, changes in species richness can

be associated with SAD changes due, for e.g., to increased numbers of common species, increased evenness (He & Legendre 2002), or increases to the size of the species pool (Fig. 2b), which results in a positive relationship between ΔS and ΔS_{PIE} (Figure 2i). Finally, if total abundance and relative abundance change in the same direction (e.g., more individuals and increased evenness, Fig. 2c), then positive pairwise relationships are expected between changes in abundance, evenness and richness (Figs. 2g, h, i).

In contrast, even if numbers of individuals increase ($\Delta N > 0$), expected gains in species richness can be constrained by decreased evenness. For example, opposing changes in total abundance and evenness can potentially result in no change to species richness (Fig. 2d), and no relationship between ΔS and ΔN (Fig. 2g). Or, if changes to the SAD are sufficiently strong, they can offset any expected gains due to more individuals (Fig. 2e), and result in a negative relationship between ΔS and ΔN (Fig. 2g). Alternatively, opposing changes to total numbers of individuals and evenness could result in a positive relationship between ΔS and ΔN if, for example, the effects of more individuals on species richness outweighs that of decreased evenness (Figure 2f).

These simplified scenarios illustrate the potential for interdependencies between component changes. In particular, they show that the signs of changes in total abundance and evenness (i.e., ΔN and ΔS_{PIE}) can strongly influence the magnitude of richness changes, and whether expected positive relationships between changes in abundance, evenness and richness are found. ΔN is associated with the IBR curve stretching or contracting along the x-axis, and ΔS_{PIE} characterizes changes that flex the curve up or down from the base along the y-axis (Olszewski 2004). When ΔN and ΔS_{PIE} have the same sign, assemblages are expected to fall into the lower left and upper

294 right quadrants of Figs. 2g-i (i.e., component changes with the same sign and positive pairwise
295 relationships). In contrast, when ΔN and ΔS_{PIE} have different signs, they can have countervailing
296 effects that constrain richness changes, the strength of their pairwise relationships with ΔS will
297 be diminished and potentially reversed, and the likelihood of assemblages falling into the upper
298 left and lower right quadrants of Figs. 2g-i increases (i.e., opposing signs and negative pairwise
299 relationships).
300
301 **Empirical relationships among total abundance, evenness and richness**
302 Next, we evaluate empirical relationships by fitting models that allow for correlations between
303 component changes to data from 1125 assemblages. Our goal for the empirical analyses was to
304 examine relationships between changing components in temporal and spatial contexts across a
305 broad range of environmental conditions. We compiled data documenting either temporal or
306 spatial variation of assemblage composition in one of either naturally-varying or perturbed
307 environmental conditions. Temporal variation quantified rates of change (i.e., per year) for each
308 component for an assemblage at a single location through time. Analyses of spatial variation
309 quantified component changes between sites in different land use categories in perturbed
310 environments, or between random pairs of sites in the naturally-varying environment.
311
312 Based on our conceptual overview, we expect pairwise relationships between abundance,
313 evenness and richness changes to be generally positive. Changes in species richness are also
314 expected to be largest for assemblages where all pairwise relationships are positive. In contrast,
315 opposing changes in total abundance and evenness (i.e., ΔN and ΔS_{PIE} have different signs) are
316 expected to constrain changes in species richness. Additionally, if local diversity changes are

317 dominated by altered total abundances and species richness, strong positive relationships
318 between ΔS and ΔN, but weaker relationships between ΔS and ΔS_n, and ΔS and ΔS_{PIE} should
319 emerge across assemblages. Alternatively, strong relationships between either ΔS and ΔS_n and/or
320 ΔS and ΔS_{PIE}, accompanied by a weaker relationship between ΔS and ΔN, would indicate that
321 changes to the SAD are the dominant component of local assemblage change.
322
323 *Temporal comparisons: natural environmental variation*
324 Temporal changes in natural assemblages at the local scale were quantified using the BioTIME
325 database (Dornelas et al. 2018). Annual rates of change (change per year) for each metric were
326 estimated with models fit to data that documents over 45 thousand species in time series with an
327 average duration of 13 years. Taxonomic groups in our analysis came from surveys in marine,
328 freshwater and terrestrial ecosystems, and included plants (and other producers), invertebrates,
329 fish, amphibians, reptiles, birds, and mammals, as well as several surveys that collected data
330 from multiple taxa. Here, we only used time series that had numerical abundance data available
331 (i.e., studies that recorded counts of the number of individuals for each species in an
332 assemblage), and our analysis included 288 studies. Locations sampled in the BioTIME database
333 document places with varying degrees of anthropogenic environmental change, but do not
334 include manipulated assemblages or before-after-control-impact studies (Dornelas et al. 2018).
335 Accordingly, we contrast the environmental variation sampled by BioTIME with assemblage
336 time series that experienced documented perturbations (see *Temporal comparisons: experimental*
337 *or natural perturbations*).
338

339 To quantify changes at the local scale within BioTIME, studies with large extents were broken
340 up into smaller cell-level time series, while still maintaining the integrity of individual studies
341 (i.e., different studies were not combined, even when samples were collected in the same grid
342 cell). We used sample-based rarefaction (Gotelli & Colwell 2001) to standardize the number of
343 samples per year for each time series (see Blowes et al. 2019 for details). For the calculation of
344 rarefied richness (S_n), the minimum total number of individuals was determined for each time
345 series, and set as the target n for which expected richness was calculated; cell-level time series
346 where $n < 5$ were discarded. This process resulted in 42,604 cell-level time series from the 288
347 studies, and we focus on the study-level estimates of change in our results and discussion.
348
349 *Temporal comparisons: experimental or natural perturbations*
350 To complement the environmental variation sampled by the BioTIME database, we searched for
351 time series data with either experimental or natural perturbations. Specifically, we queried the
352 U.S. LTER network using the Data Portal of the Environmental Data Initiative
353 (https://portal.edirepository.org/nis/home.jsp) with the search terms 'experiment' and 'time' and
354 'abundance'. Records returned were checked to confirm that samples documented assemblages
355 of similar species collected with the same methodology, and following data standardization (i.e.,
356 minimum of five individuals per sample, and standardization of sample effort through time), our
357 analysis included 11 studies (see Appendix S1: *Temporal comparisons: experimental or natural*
358 *perturbations* for references), and annual rates of change (i.e., per year) were estimated for 63
359 study-treatment combinations; rates of change for all treatments (including controls) were
360 quantified in our analyses. Natural and experimental treatments included changes due to

361 warming, eutrophication, fire, grazing, restoration, severe storms or other disturbances, and kelp
362 removal. Taxonomic groups included algae, plants, invertebrates, fish, birds, and mammals.
363
364 *Spatial comparisons: natural environmental variation*
365 We combined two existing compilations of data to examine spatial patterns of biodiversity
366 change in relatively natural environmental contexts. The CESTES database (Jeliazkov et al.
367 2019) contains assemblage data from studies that sampled species at multiple sites (it also
368 includes information on traits and environment that we do not use here); we removed studies
369 with explicit human impacts identified as an environmental feature, and our analysis included 19
370 studies that sampled terrestrial, freshwater and marine assemblages from a number of taxonomic
371 groups (birds, plants, insects, macroinvertebrates, fishes and mammals). McGill (2011b)
372 compiled datasets with two or more local assemblages containing species abundance data; we
373 removed studies documenting disturbances and other perturbations, resulting in 32 studies being
374 retained. From the combined 51 studies, those with many sites were randomly subsampled down
375 to ten sites so that they did not dominate the results. Within each study, an arbitrary site was
376 assigned as the 'reference' site, and change was quantified between every site and the reference
377 within studies; our analysis included a total of 356 spatial comparisons.
378
379 *Spatial comparisons: anthropogenic perturbations*
380 To quantify spatial differences in biodiversity due to anthropogenic land use, we used the
381 PREDICTS database (Hudson et al. 2017). We used the 2016 release of the database
382 (downloaded from https://data.nhm.ac.uk/dataset/the-2016-release-of-the-predicts-database on
383 10th July 2020). We limited our analyses to studies with abundance data for individuals, and

384 those with known land use categories (primary vegetation, mature secondary vegetation,
385 intermediate secondary vegetation, plantation forest, cropland, pasture, and urban); studies where
386 land use was not recorded were omitted. This resulted in 237 combinations of source ID and
387 study (some sources had multiple studies, denoted SS in the database), and 418 estimates of
388 change relative to the reference land use (primary vegetation) category.
389
390 *Statistical models*
391 To estimate changes in the different metrics whilst accounting for expected correlations between
392 them, we fit multivariate multilevel models to the data. Similar to the way univariate multilevel
393 (also called hierarchical or mixed-effects) models fit to a single response can allow varying (also
394 called random) intercepts and slopes to be correlated, this approach estimates changes in all
395 components simultaneously whilst allowing for (and estimating) correlations between them.
396 Response distributions for all metrics were chosen to ensure changes were estimated on similar
397 measurement scales, and because all metrics take only positive values, log response scales were
398 used for all components.
399
400 For the *Temporal comparisons: natural environmental variation* data, total abundance (N) was
401 fit with a model that assumed a lognormal distribution and identity link function, and Poisson
402 distributions with log link functions were fit to S_n, S_{PIE} and S; Poisson distributions were chosen
403 for S_n and S_{PIE} values rounded to integers based on visual assessments that showed lognormal
404 models fit to raw S_n and S_{PIE} values greatly underpredicted the density of ones in the data. For the
405 *Temporal comparisons: experimental or natural perturbations* data, S was no longer an integer
406 value after standardizing sampling effort, and all metrics were fit with models that assumed

407 lognormal distributions and identity link functions. Both spatial data sets were fit with models
408 that assumed lognormal distributions and identity link functions for total abundance (N), rarefied
409 richness (S_n) and evenness (S_{PIE}), and a Poisson distribution and log-link function for species
410 richness (S).
411
412 The *Temporal comparisons: natural environmental variation* models included non-varying
413 intercepts and slopes for year, and varying intercepts and slopes for studies and cells for all
414 responses. To allow for correlations between changes in the different responses, varying study-
415 and cell-level parameters for all responses were drawn from a single multivariate normal
416 distribution for each level (i.e., one for studies, one for cells; see Appendix S1: *Temporal*
417 *comparisons: natural environmental variation* for equations). The models fit to the *Temporal*
418 *comparisons: experimental or natural perturbations* data similarly included non-varying
419 intercepts and slopes for year, and had varying intercepts for study, site and block fitted
420 separately for each response. For these data, correlations between changes in the different
421 responses were modeled by drawing varying intercepts and slopes for each combination of
422 treatment and study for all responses from a single multivariate normal distribution (see
423 Appendix S1: *Temporal comparisons: experimental or natural perturbations* for equations).
424
425 The models fit to the *Spatial comparisons: natural environmental variation* data included non-
426 varying intercepts for data source (i.e., CESTES and McGill). Correlations between the different
427 responses were modeled by assuming varying intercepts and slopes (representing the reference
428 site and departures for all other sites from the reference, respectively) for each study and
429 response came from a single multivariate normal distribution; over-dispersion in the richness

response was modeled using an observation-level varying intercept (see Appendix S1: *Spatial comparisons: natural environmental variation* for equations). Models fit to the *Spatial comparisons: anthropogenic perturbations* data included non-varying intercepts and slopes (representing the reference [primary vegetation] category and departures from the reference for each land use category, respectively), and varying intercepts for sites and blocks were modeled separately for each response. Correlations between changes in the different responses were modeled by assuming that varying intercepts and slopes (as per the non-varying intercepts and slopes) for each combination of source and study and each response came from a single multivariate normal distribution (see Appendix S1: *Spatial comparisons: anthropogenic perturbations* for equations).

All statistical models were estimated using the Hamiltonian Monte Carlo (HMC) sampler Stan (Carpenter et al. 2017), and coded using the 'brms' package (Burkner 2017). Details of all model specifications, and the iterations and warmup periods are provided in the Appendix, as are the priors (which were weakly regularizing). Visual inspection of the HMC chains and model diagnostics (Rhat < 1.05) showed good mixing of chains and convergence, and model adequacy assessed visually using posterior predictive checks showed that the models were able to make predictions similar to the empirical data (see Appendix Figure: S1-4). Code for all analyses is available at https://github.com/sablowes/MulticomponentBioChange, and will be archived following publication.

Results

Temporal changes in perturbed environments had the highest percentage of assemblages with at least one component trend (ΔN, ΔS_n, ΔS_{PIE}, or ΔS) that differed from zero (44%), followed by spatial comparisons across land use categories (29%), temporal changes (21%) and spatial comparisons in naturally varying environments (12%). Component changes that differed from zero showed broadly similar patterns across datasets, with one exception: trends differing from zero for multiple components were less common for spatial comparisons between assemblages in naturally varying environments (Appendix S1: Figure S5).

Pairwise relationships between changing components were typically positive (i.e., had the same sign), though exceptions to this general pattern were found for all data sources (Figure 3). For assemblages where ΔN and ΔS_{PIE} had the same sign (though not necessarily differing statistically from zero), richness changes were typically larger in magnitude (Figure 3). In contrast, assemblages where ΔN and ΔS_{PIE} had opposing signs typically exhibited changes in richness that were smaller in magnitude (Figure 3). This tendency for countervailing changes in abundance and evenness to constrain richness changes was most apparent for spatial comparisons between different land use categories (Figure 3j-l), and there was a high proportion of assemblages that were growing in size ($\Delta N > 0$) but with declining species richness ($\Delta S < 0$; Figure 3j), associated with declining evenness ($\Delta S_{PIE} < 0$).

The strongest relationships were found for components changing through time, and relationships between richness and changes in the SAD -- rarefied richness (Figs. 3b, e) and evenness (Figs. 3c, f; Figs. 4a, b) -- were stronger than those between changes in richness and total abundance (Figs. 3a, c; Figs. 4a, b). Spatial comparisons had generally weak relationships overall. No strong

relationships between changing components emerged for comparisons in natural environments (Figs. 3g-i; Fig. 4c), and only weakly positive relationships between changes in abundance, evenness and richness were found in comparisons between primary vegetation and different land use categories (Figure 3j-l, Figure 4d).

Temporal changes in naturally varying assemblages were roughly centered on zero for all metrics (Figure 3a-c). Across assemblages, altered numbers of individuals and species richness changes had a moderately positive relationship (Figure 4a), weakened predominantly by assemblages that had opposing abundance and evenness relationships (Figure 3a). In contrast, relationships between changes in species richness and rarefied richness, and between richness changes and evenness changes were strong (Figure 4a). Assemblages in perturbed environments had slightly positive temporal trends on average in all components (Figure 3d-f). Across assemblages, ΔS and ΔN (Figure 3d, 4b) and ΔS and ΔS_{PIE} (Figure 3f, 4b) had relatively weak positive relationships, whereas ΔS and ΔS_{n} (Figure 3e, 4b) showed a strong positive relationship.

Spatial comparisons in naturally varying environments exhibited highly heterogeneous patterns of change centered around zero for all metrics (Figure 3g-i). Decoupled component changes meant that relationships between them were generally absent or weak across assemblages (Figure 4c). Spatial comparisons between assemblages in primary vegetation versus those in different land use categories were also highly heterogeneous, though there were typically fewer individuals, less even assemblages and fewer species relative to primary vegetation (Figure 3j-l). Across assemblages, land use change was typically associated with relatively weak positive relationships between changes in the components of local diversity (Figure 4d).

Discussion

Our conceptual overview using individual-based rarefaction curves clearly shows how the expectation of positive pairwise relationships between changes in abundance, evenness and richness arises. If curves stretch or contract, we expect positive relationships between changes in total abundance and richness. Similarly, if curves flex upwards or downwards, positive relationships between changes in evenness and richness are expected. Rarefaction curves also show how contrasting signs of changes in abundance and evenness can strongly determine the magnitude of richness changes, and determine whether positive relationships between changes in richness and the other components (abundance and evenness) are likely. Both these predictions were generally well supported by our empirical analyses. Relationships between changes in abundance, evenness and richness were generally positive, and richness changes were typically greater for assemblages with strictly positive pairwise relationships. Countervailing changes in total abundance and evenness, where found, often constrained the magnitude of changes in species richness, and acted to weaken relationships between ΔN and ΔS, and ΔS_{PIE} and ΔS. Spatial comparisons had the most heterogeneous relationships between changes in abundance, evenness, and richness, and in relatively natural environments changes were sufficiently decoupled that no strong relationships emerged across assemblages. In contrast, strong positive correlations between temporal changes in species richness (ΔS) and changes in metrics associated with altered SADs (ΔS_{n}, ΔS_{PIE}) emerged across assemblages. These temporal results show strong support for the prediction that variation in relative abundances can dominate local variation in biodiversity (Chapin et al. 2000), even when human impacts are less direct.

Variation in assemblage size does not dominate local diversity change

522 Overall, only ~2% of assemblages in this study (22 of 1125) had changes consistent with a
523 strong 'sampling' effect on changes in species richness (i.e., ΔN & ΔS having the same sign, and
524 being the only changes different from zero). This finding complements existing evidence
525 showing that despite many tests, empirical evidence for the more-individuals hypothesis
526 (Srivastava & Lawton 1998) remains equivocal (Storch et al 2018, Vagle & McCain 2020).
527 While both (species-level) population variability and variation associated with sampling (Vagle
528 & McCain 2020) likely contribute to the weak response of species richness to variation in the
529 total number of individuals, our results are broadly consistent with previous syntheses showing
530 that broad-scale spatial variation in richness was rarely driven simply by variation in the numbers
531 of individuals (Currie et al. 2004, Storch et al 2018). Our results indicate that variation in local
532 diversity, through time or from site-to-site, is not due to changes in assemblage size passively
533 sampling more or less from a static SAD. Instead, we show that variation in local biodiversity
534 can be strongly influenced by changes to species' relative abundances. These changes can be
535 occurring at multiple scales (Hillebrand et al. 2008, Blowes et al. 2020), and could reflect altered
536 local environmental conditions (e.g., altered resource or habitat availability and diversity,
537 eutrophication, local harvest or exploitation), or changes at broader scales that alter the species
538 pool (via species additions or subtractions).
539
540 Our general result showing that variation in the total abundance of an assemblage through time
541 or space is often decoupled from changes in metrics of biodiversity such as species richness also
542 cautions against making "apples to oranges" comparisons in the context of quantifying
543 biodiversity change. For example, some estimates of change are based on either population-level
544 abundance (e.g., Living Planet Index, WWF 2020), or assemblage-level abundance (e.g., insect

545 declines; Wagner 2000, van Klink et al. 2020), whereas other change estimates are based on
546 patterns of the number or identity of species present (e.g., Dornelas et al. 2014, Newbold et al.
547 2015). Our results show that assuming abundance and richness changes are strongly correlated
548 will often be an oversimplification. Moreover, the importance of altered relative abundances for
549 local biodiversity variation means that biodiversity change estimates will frequently depend on
550 whether changes in species relative abundances influence the metrics used (see e.g., Antão et al.
551 2020b).
552
553 *Contrasting component relationships between temporal changes versus spatial comparisons of*
554 *biodiversity*
555 Relationships between changing components of biodiversity showed strikingly different patterns
556 between temporal changes and spatial comparisons. Moreover, these differences were generally
557 greater than those found between naturally-varying and perturbed assemblages, for either
558 temporal changes or spatial comparisons.
559
560 Pairwise relationships between changes in abundance, evenness and richness were typically
561 weak for spatial comparisons. Decoupling was greatest, and pairwise relationships weakest, for
562 changes between sites experiencing relatively natural environmental variation. However, given
563 our simple conceptual framework shows that some degree of interdependence cannot be avoided,
564 we caution against overinterpreting the relative independence of these component changes, and
565 further analyses examining component change relationships along continuous spatial gradients
566 are warranted. Indeed, evenness and richness are never numerically independent (Jost 2010), and
567 the weak overall relationship between changes in richness and evenness for these data was in

568 part due to assemblages with countervailing changes in abundance and evenness. Most
569 importantly, these highly variable component changes further emphasize the need for a holistic
570 approach to quantifying biodiversity change (Chase et al. 2018, Avolio et al. 2021).
571
572 Our prediction that the signs of changes in abundance and evenness can strongly determine the
573 magnitude of richness changes was most evident in the spatial contrasts between primary
574 vegetation and other land use categories (Newbold et al. 2015, 2020). Assemblages with the
575 greatest declines in abundance and evenness had the greatest richness declines. In contrast, when
576 abundance and evenness changes had opposing signs, richness changes were tempered. Indeed,
577 countervailing abundance and evenness changes were frequently associated with components
578 other than species richness (i.e., ΔN, ΔS_n, and/or ΔS_{PIE}) having a trend that differed from zero
579 across all data sources (Appendix S1: Table S1). This highlights that even apparently decoupled
580 or weakly correlated component changes have interdependencies that can remain important
581 determinants of observed changes.
582
583 In contrast to assemblage change between sites, there was strong coupling between species
584 richness and SAD changes through time. In particular, the strength of the relationship between
585 ΔS_n and ΔS resulted in estimates of change being similar for most assemblage time series in
586 relatively natural environments (Figure 3b). In some cases, this occurred despite countervailing
587 changes in total abundance and evenness (Figure 3a, b). For assemblages where abundance and
588 evenness changed in the same direction, similar estimates of ΔS_n and ΔS indicate that abundance
589 changes were occurring along a relatively flat region of the individual-based rarefaction curve.
590 This shows that changes to the total number of individuals need not strongly influence species

richness, even where signs are the same and they have a positive relationship. The strong association between richness changes and altered relative abundances has important implications for examining causes and/or consequences of biodiversity change (Hillebrand et al. 2008, Crowder et al. 2010). Even where the expected positive relationships between abundance, evenness and richness are found, we can more fully understand assemblage changes when all component changes are examined simultaneously.

While both approaches, time series and spatial comparisons (or space-for-time substitutions), have contributed to our understanding of biodiversity change, the relative merits of each for our understanding of ecological dynamics has not been discussed much (Adler et al. 2020). The largely decoupled component changes found here for spatial comparisons suggest that too much focus on average changes across assemblages, such as those in total abundance or in species richness, risks masking highly heterogeneous changes occurring within assemblages in multiple components. Moreover, decoupled, heterogeneous component changes complicate using spatial comparisons to infer temporal changes. The smaller effect sizes found here for time series indicates greater inertia compared to site-to-site variation. More generally, the strong role of changes to the SAD for variation in local biodiversity suggests that deepening our understanding of altered patterns of relative abundance across scales represents an important direction for future theoretical and empirical work. Here our focus has been on numerical relationships between component changes, and using process-based models (e.g., Thompson et al. 2020) to examine how altered metacommunity dynamics impact patterns of relative abundance across scales could help our understanding how different processes impact component relationships. Similarly, empirical studies could ask whether local environmental changes are affecting evenness, or if

614 changes occurring at broader spatial scales are impacting the size of species pool and the
615 regional SAD?
616
617 *Conclusions*
618 We found strong correlations between changes in the SAD and species richness changes through
619 time, whereas relationships between abundance and richness changes for both temporal and
620 spatial diversity variation were generally weak. Our findings confirm that altered species relative
621 abundances, and/or changes to the size of the species pool, often strongly influence local
622 diversity change (Chapin et al. 2010), even where human impacts are less direct. However, our
623 results also reinforce cautions against examining changes to any one component of biodiversity
624 change in isolation (e.g., Wilsey et al. 2005, Chase et al. 2018, Avolio et al. 2021).
625
626 To be most useful, quantifying (co)variation in the different components of biodiversity needs to
627 be done coherently. Individual-based rarefaction curves and associated metrics can provide an
628 intuitive and illustrative characterization of relationships among changing components of local
629 biodiversity. Whilst ecologists are increasingly looking beyond species richness to quantify
630 biodiversity change (e.g., Dornelas et al. 2014, Hillebrand et al. 2018), different components of
631 biodiversity and its change within assemblages are most often analyzed independently, and
632 frequently with metrics lacking conceptual unity. Conceptually and empirically, our results
633 emphasize that changes to the most frequently quantified aspects of biodiversity, including
634 changes to the numbers of individuals, and the relative abundance and total number of species
635 are highly interdependent. Examining how within-assemblage component changes covary with
636 potential drivers could reveal insights masked by independent aggregate estimates of change

637 across assemblages, and provide new information for understanding biodiversity change in the
638 Anthropocene.
639

640 **Acknowledgements**

641 SAB thanks the Biodiversity Synthesis group at iDiv for contructive feedback at various stages
642 of the project. SAB, TE, AS, and JMC were supported by the German Centre for Integrative
643 Biodiversity Research (iDiv) Halle-Jena-Leipzig, funded by the German Research Foundation
644 (FZT 118).
645

646 **References**

647 Antão, L.H., Bates, A.E., Blowes, S.A., Waldock, C., Supp, S.R., Magurran, A.E., Dornelas, M.,
648 Schipper, A.M., 2020a. Temperature-related biodiversity change across temperate marine and
649 terrestrial systems. Nature ecology & evolution 4, 927–933.
650 Antão, L.H., Pöyry, J., Leinonen, R., Roslin, T., 2020b. Contrasting latitudinal patterns in
651 diversity and stability in a high-latitude species-rich moth community. Global Ecology and
652 Biogeography 29, 896–907.
653 Avolio, M.L., Komatsu, K.J., Collins, S.L., Grman, E., Koerner, S.E., Tredennick, A.T., Wilcox,
654 K.R., Baer, S., Boughton, E.H., Britton, A.J., 2021. Determinants of community
655 compositional change are equally affected by global change. Ecology Letters 24, 1892–1904.
656 Blowes, S.A., Chase, J.M., Di Franco, A., Frid, O., Gotelli, N.J., Guidetti, P., Knight, T.M., May,
657 F., McGlinn, D.J., Micheli, F., 2020. Mediterranean marine protected areas have higher
658 biodiversity via increased evenness, not abundance. Journal of Applied Ecology 57, 578–589.

Blowes, S.A., Supp, S.R., Antão, L.H., Bates, A., Bruelheide, H., Chase, J.M., Moyes, F., Magurran, A., McGill, B., Myers-Smith, I.H., Winter, M., Bjorkman, A.D., Bowler, D.E., Byrnes, J.E., Gonzalez, A., Hines, J., Isbell, F., Jones, H.P., Navarro, L.M., Thompson, P.L., Vellend, M., Waldock, C., Dornelas, M., 2019. The geography of biodiversity change in marine and terrestrial assemblages. Science 366, 339–345.

Bolker, B.M., 2008. Ecological models and data in R. Princeton University Press.

Bürkner, P.-C., 2017. brms: An R package for Bayesian multilevel models using Stan. Journal of Statistical Software 80, 1–28.

Carpenter, B., Gelman, A., Hoffman, M.D., Lee, D., Goodrich, B., Betancourt, M., Brubaker, M., Guo, J., Li, P., Riddell, A., 2017. Stan: A probabilistic programming language. Journal of Statistical Software 76.

Caswell, H., 1976. Community structure: a neutral model analysis. Ecological monographs 46, 327–354.

Cayuela, L., Gotelli, N.J., Colwell, R.K., 2015. Ecological and biogeographic null hypotheses for comparing rarefaction curves. Ecological Monographs 85, 437–455.

Chao, A., Gotelli, N.J., Hsieh, T.C., Sander, E.L., Ma, K.H., Colwell, R.K., Ellison, A.M., n.d. Rarefaction and extrapolation with Hill numbers: a framework for sampling and estimation in species diversity studies. Ecology 84, 45–67.

Chao, A., Jost, L., 2012. Coverage-based rarefaction and extrapolation: standardizing samples by completeness rather than size. Ecology 93, 2533–2547.

Chapin Iii, F.S., Zavaleta, E.S., Eviner, V.T., Naylor, R.L., Vitousek, P.M., Reynolds, H.L., Hooper, D.U., Lavorel, S., Sala, O.E., Hobbie, S.E., 2000. Consequences of changing biodiversity. Nature 405, 234–242.

682 Chase, J.M., Blowes, S.A., Knight, T.M., Gerstner, K., May, F., 2020. Ecosystem decay
683 exacerbates biodiversity loss with habitat loss. Nature 584, 238–243.
684 Chase, J.M., Knight, T.M., 2013. Scale-dependent effect sizes of ecological drivers on
685 biodiversity: why standardised sampling is not enough. Ecol Lett 16, 17–26.
686 Chase, J.M., McGill, B.J., McGlinn, D.J., May, F., Blowes, S.A., Xiao, X., Knight, T.M.,
687 Purschke, O., Gotelli, N.J., 2018. Embracing scale-dependence to achieve a deeper
688 understanding of biodiversity and its change across communities. Ecol Lett 21, 1737–1751.
689 Chase, J.M., McGill, B.J., Thompson, P.L., Antão, L.H., Bates, A.E., Blowes, S.A., Dornelas,
690 M., Gonzalez, A., Magurran, A.E., Supp, S.R., Winter, M., Bjorkman, A.D., Bruelheide, H.,
691 Byrnes, J.E., Sarmento Cabral, J., Elahi, R., Gomez, C., Guzman, H.M., Isbell, F., Myers-
692 Smith, I.H., Jones, H.P., Hines, J., Vellend, M., Waldock, C., O'Connor, M., 2019. Species
693 richness change across spatial scales. Oikos 1–13.
694 Coleman, B.D., Mares, M.A., Willig, M.R., Hsieh, Y.-H., 1982. Randomness, area, and species
695 richness. Ecology 63, 1121–1133.
696 Connell, J.H., 1978. Diversity in tropical rain forests and coral reefs. Science 199, 1302–1310.
697 Connor, E.F., McCoy, E.D., 1979. The statistics and biology of the species-area relationship. The
698 American Naturalist 113, 791–833.
699 Crowder, D.W., Northfield, T.D., Strand, M.R., Snyder, W.E., 2010. Organic agriculture
700 promotes evenness and natural pest control. Nature 466, 109–112.
701 Currie, D.J., 1991. Energy and large-scale patterns of animal-and plant-species richness. Am Nat
702 27–49.

Currie, D.J., Mittelbach, G.G., Cornell, H.V., Field, R., Guégan, J.-F., Hawkins, B.A., Kaufman, D.M., Kerr, J.T., Oberdorff, T., O'Brien, E., 2004. Predictions and tests of climate-based hypotheses of broad-scale variation in taxonomic richness. Ecology letters 7, 1121–1134.

Daskalova, G.N., Myers-Smith, I.H., Bjorkman, A.D., Blowes, S.A., Supp, S.R., Magurran, A.E., Dornelas, M., 2020a. Landscape-scale forest loss as a catalyst of population and biodiversity change. Science 368, 1341–1347.

Daskalova, G.N., Myers-Smith, I.H., Godlee, J.L., 2020b. Rare and common vertebrates span a wide spectrum of population trends. Nature Communications 4394.

Díaz, S., Settele, J., Brondízio, E.S., Ngo, H.T., Agard, J., Arneth, A., Balvanera, P., Brauman, K.A., Butchart, S.H., Chan, K.M., 2019. Pervasive human-driven decline of life on Earth points to the need for transformative change. Science 366.

Dornelas, M., Antao, L.H., Moyes, F., Bates, A.E., Magurran, A.E., Adam, D., Akhmetzhanova, A.A., Appeltans, W., Arcos, J.M., Arnold, H., 2018. BioTIME: A database of biodiversity time series for the Anthropocene. Glob Ecol Biogeogr 27, 760–786.

Dornelas, M., Gotelli, N.J., McGill, B., Shimadzu, H., Moyes, F., Sievers, C., Magurran, A.E., 2014. Assemblage time series reveal biodiversity change but not systematic loss. Science 344, 296–299.

Dornelas, M., Gotelli, N.J., Shimadzu, H., Moyes, F., Magurran, A.E., McGill, B.J., 2019. A balance of winners and losers in the Anthropocene. Ecol Lett 22, 847–854.

Fisher, R.A., Corbet, A.S., Williams, C.B., 1943. The relation between the number of species and the number of individuals in a random sample of an animal population. The Journal of Animal Ecology 42–58.

Gaston, K.J., 2000. Global patterns in biodiversity. Nature 405, 220–227.

Gotelli, N.J., Colwell, R.K., 2001. Quantifying biodiversity: procedures and pitfalls in the measurement and comparison of species richness. Ecol Lett 4, 379–391.

He, F., Legendre, P., 2002. Species diversity patterns derived from species–area models. Ecology 83, 1185–1198.

Hill, M.O., 1973. Diversity and evenness: a unifying notation and its consequences. Ecology 54, 427–432.

Hillebrand, H., Bennett, D.M., Cadotte, M.W., 2008. Consequences of dominance: a review of evenness effects on local and regional ecosystem processes. Ecology 89, 1510–1520.

Hillebrand, H., Blasius, B., Borer, E.T., Chase, J.M., Downing, J.A., Eriksson, B.K., Filstrup, C.T., Harpole, W.S., Hodapp, D., Larsen, S., 2018. Biodiversity change is uncoupled from species richness trends: Consequences for conservation and monitoring. Journal of Applied Ecology 55, 169–184.

Hudson, L.N., Newbold, T., Contu, S., Hill, S.L., Lysenko, I., De Palma, A., Phillips, H.R., Alhusseini, T.I., Bedford, F.E., Bennett, D.J., 2017. The database of the Predicts (Projecting responses of ecological diversity in changing terrestrial systems) project. Ecology and Evolution 7, 145–188.

Hughes, A.R., Byrnes, J.E., Kimbro, D.L., Stachowicz, J.J., 2007. Reciprocal relationships and potential feedbacks between biodiversity and disturbance. Ecology letters 10, 849–864.

Hurlbert, S.H., 1971. The nonconcept of species diversity: a critique and alternative parameters. Ecology 52, 577–586.

Jeliazkov, A., Mijatovic, D., Chantepie, S., Andrew, N., Arlettaz, R., Barbaro, L., Barsoum, N., Bartonova, A., Belskaya, E., Bonada, N., 2020. A global database for metacommunity ecology, integrating species, traits, environment and space. Scientific data 7, 1–15.

749 Jones, F.A., Magurran, A.E., 2018. Dominance structure of assemblages is regulated over a
750 period of rapid environmental change. Biology letters 14, 20180187.
751 Jost, L., 2007. Partitioning diversity into independent alpha and beta components. Ecology 88,
752 2427–2439.
753 Jost, L., 2006. Entropy and diversity. Oikos 113, 363–375.
754 Kreft, H., Jetz, W., Mutke, J., Kier, G., Barthlott, W., 2008. Global diversity of island floras from
755 a macroecological perspective. Ecology letters 11, 116–127.
756 Latham, R.E., Ricklefs, R.E., 1993. Global patterns of tree species richness in moist forests:
757 energy-diversity theory does not account for variation in species richness. Oikos 325–333.
758 Leung, B., Hargreaves, A.L., Greenberg, D.A., McGill, B., Dornelas, M., Freeman, R., 2020.
759 Clustered versus catastrophic global vertebrate declines. Nature 588, 267–271.
760 MacArthur, R.H., 1965. Patterns of species diversity. Biological reviews 40, 510–533.
761 Magurran, A.E., McGill, B.J., 2011. Biological diversity: frontiers in measurement and
762 assessment. Oxford University Press.
763 May, F., Gerstner, K., McGlinn, D.J., Xiao, X., Chase, J.M., 2018. mobsim: An R package for
764 the simulation and measurement of biodiversity across spatial scales. Methods in Ecology and
765 Evolution 9, 1401–1408.
766 McGill, B.J., 2011a. Linking biodiversity patterns by autocorrelated random sampling. Am J Bot
767 98, 481–502.
768 McGill, B.J., 2011b. Species abundance distributions, in: Biological Diversity: Frontiers In
769 Measurement & Assessment (Eds Magurran, A. & McGill, B.). Oxford University Press, pp.
770 105–122.

McGill, B.J., Etienne, R.S., Gray, J.S., Alonso, D., Anderson, M.J., Benecha, H.K., Dornelas, M., Enquist, B.J., Green, J.L., He, F., Hurlbert, A.H., Magurran, A.E., Marquet, P.A., Maurer, B.A., Ostling, A., Soykan, C.U., Ugland, K.I., White, E.P., 2007. Species abundance distributions: moving beyond single prediction theories to integration within an ecological framework. Ecol Lett 10, 995–1015.

McGlinn, D.J., Xiao, X., May, F., Gotelli, N.J., Engel, T., Blowes, S.A., Knight, T.M., Purschke, O., Chase, J.M., McGill, B.J., 2019. Measurement of Biodiversity (MoB): A method to separate the scale-dependent effects of species abundance distribution, density, and aggregation on diversity change. Methods in Ecology and Evolution 10, 258–269.

McKinney, M.L., Lockwood, J.L., 1999. Biotic homogenization: a few winners replacing many losers in the next mass extinction. Trends in ecology & evolution 14, 450–453.

Menge, B.A., Berlow, E.L., Blanchette, C.A., Navarrete, S.A., Yamada, S.B., 1994. The keystone species concept: variation in interaction strength in a rocky intertidal habitat. Ecological monographs 64, 249–286.

Miller, A.D., Roxburgh, S.H., Shea, K., 2011. How frequency and intensity shape diversity–disturbance relationships. Proceedings of the National Academy of sciences 108, 5643–5648.

Mittelbach, G.G., Steiner, C.F., Scheiner, S.M., Gross, K.L., Reynolds, H.L., Waide, R.B., Willig, M.R., Dodson, S.I., Gough, L., 2001. What is the observed relationship between species richness and productivity? Ecology 82, 2381–2396.

Newbold, T., Hudson, L.N., Contu, S., Hill, S.L., Beck, J., Liu, Y., Meyer, C., Phillips, H.R., Scharlemann, J.P., Purvis, A., 2018. Widespread winners and narrow-ranged losers: Land use homogenizes biodiversity in local assemblages worldwide. PLoS biology 16, e2006841.

Newbold, T., Hudson, L.N., Hill, S.L., Contu, S., Lysenko, I., Senior, R.A., Börger, L., Bennett, D.J., Choimes, A., Collen, B., 2015. Global effects of land use on local terrestrial biodiversity. Nature 520, 45–50.

Newbold, T., Oppenheimer, P., Etard, A., Williams, J.J., 2020. Tropical and Mediterranean biodiversity is disproportionately sensitive to land-use and climate change. Nature Ecology & Evolution 4, 1630–1638.

Olszewski, T.D., 2004. A unified mathematical framework for the measurement of richness and evenness within and among multiple communities. Oikos 104, 377–387.

Paine, R.T., 1974. Intertidal community structure. Oecologia 15, 93–120.

Palmer, M.W., Clark, D.B., Clark, D.A., 2000. Is the number of tree species in small tropical forest plots nonrandom? Community Ecology 1, 95–101.

Preston, F.W., 1962. The canonical distribution of commonness and rarity: Part I. Ecology 43, 185–215.

Rosenberg, K.V., Dokter, A.M., Blancher, P.J., Sauer, J.R., Smith, A.C., Smith, P.A., Stanton, J.C., Panjabi, A., Helft, L., Parr, M., 2019. Decline of the North American avifauna. Science 366, 120–124.

Rosenzweig, M.L., 1995. Species diversity in space and time. Cambridge University Press.

Scheiner, S.M., Willig, M.R., 2005. Developing unified theories in ecology as exemplified with diversity gradients. The American Naturalist 166, 458–469.

Shmida, A.V.I., Wilson, M.V., 1985. Biological determinants of species diversity. Journal of biogeography 1–20.

Soininen, J., Passy, S., Hillebrand, H., 2012. The relationship between species richness and evenness: a meta-analysis of studies across aquatic ecosystems. Oecologia 169, 803–809.

Srivastava, D.S., Lawton, J.H., 1998. Why more productive sites have more species: an experimental test of theory using tree-hole communities. The American Naturalist 152, 510–529.

Stirling, G., Wilsey, B., 2001. Empirical relationships between species richness, evenness, and proportional diversity. The American Naturalist 158, 286–299.

Storch, D., Bohdalková, E., Okie, J., 2018. The more-individuals hypothesis revisited: the role of community abundance in species richness regulation and the productivity–diversity relationship. Ecol Lett 21, 920–937.

Tilman, D., 1982. Resource competition and community structure. Princeton University Press.

Vagle, G.L., McCain, C.M., n.d. Natural population variability may be masking the more-individuals hypothesis. Ecology 101, e03035.

Van Klink, R., Bowler, D.E., Gongalsky, K.B., Swengel, A.B., Gentile, A., Chase, J.M., 2020. Meta-analysis reveals declines in terrestrial but increases in freshwater insect abundances. Science 368, 417–420.

Vilà, M., Espinar, J.L., Hejda, M., Hulme, P.E., Jarošík, V., Maron, J.L., Pergl, J., Schaffner, U., Sun, Y., Pyšek, P., 2011. Ecological impacts of invasive alien plants: a meta-analysis of their effects on species, communities and ecosystems. Ecology letters 14, 702–708.

Wagner, D.L., 2020. Insect declines in the Anthropocene. Annual review of entomology 65, 457–480.

Whittaker, R.J., Willis, K.J., Field, R., 2001. Scale and species richness: towards a general, hierarchical theory of species diversity. Journal of biogeography 28, 453–470.

Wright, D.H., 1983. Species-energy theory: an extension of species-area theory. Oikos 496–506.

838 WWF, 2020. Living Planet Report 2020-Bending the curve of biodiversity loss. World Wildlife
839 Fund, Gland, Switzerland.
840 Zhang, Y., Chen, H.Y., Reich, P.B., 2012. Forest productivity increases with evenness, species
841 richness and trait variation: a global meta-analysis. Journal of ecology 100, 742–749.
842

Figure 1: (a) Individual-based rarefaction (IBR) curves for two hypothetical assemblages, showing the four components we use to quantify change (N, S, S_n, PIE). We visualize relationships between these four components of the IBR curve by plotting: (b) changes in species richness (ΔS) as a function of altered numbers of individuals (ΔN), (c) changes in species richness (ΔS) as a function of changes in rarefied richness (ΔS_n), and (d) changes in species richness (ΔS) as a function of the numbers equivalent conversion of the Probability of Interspecific Encounter (ΔS_{PIE}). We show ΔPIE on the figure to illustrate changes of the PIE (it is equivalent to the slope at the base of the curve) with the IBR, but use the numbers equivalent transformation (ΔS_{PIE}) in all analyses. Points on panels (b, c, and d) show changes between the two hypothetical assemblages, with the reference assemblage depicted by the grey line.

Figure 2: Conceptual illustrations of potential pathways of local assemblage diversity change and corresponding relationships between component changes. Starting from a reference assemblage (depicted with grey rarefaction curves), diversity change can be due to (a) more individuals only, (b) changes to the species abundance distribution only (e.g., increased species pool size or increased evenness), or (c) changes in total abundance and the SAD that result in positive pairwise relationships between ΔN, ΔS_n, ΔS_{PIE}, and ΔS. However, if the signs of ΔN and ΔS_{PIE} differ, their relationships with ΔS weaken and species richness can (d) remain static, (e) decrease or (f) increase. We visualize pairwise relationships between component changes for each scenario (i.e., the different shaped symbols) using: (g) changes in species richness as a function of changes to the number of individuals, (h) changes in species richness as a function of changes in rarefied richness, and (i) changes in species richness as a function of changes in evenness.

866 **Figure 3**: Empirical relationships between four components of local diversity change. Change in
867 species richness as a function of changes in the numbers of individuals (left column), rarefied
868 richness (middle column), and evenness (right column) for (a-c) study-level estimates of
869 temporal changes in naturally varying environments; (d-f) estimates of temporal change for
870 combinations of study and treatment in perturbed environments; (g-i) estimates of spatial
871 changes within studies from an arbitrary reference site along natural environmental gradients;
872 and, (j-l) estimates of spatial change within studies between primary vegetation and different
873 land use categories. Colored concentration ellipses show the confidence interval (5 and 95%) of
874 the posterior distributions. Dotted grey lines are x and y = 0, and x = y. See Appendix S1: Figure
875 S6 for remaining pairwise relationships. Scale of x- and y-axes vary between panels; one
876 estimate with $\Delta\log(N) = -1.79$, $\Delta\log(S) = -3.77$, $\Delta\log(S_n) = -3.23$, $\Delta\log(S_{PIE}) = -3.21$, removed
877 from (j-l) for clarity.
878
879 **Figure 4**: Component correlations among studies within each data source. Density plots for the
880 posterior distribution of pairwise correlations between component changes for (a) temporal
881 comparison in naturally varying environments, (b) temporal comparisons in perturbed
882 environments, (c) spatial comparisons along natural gradients, and (d) spatial comparisons
883 between different land use categories. Correlations estimated separately for sites and land use
884 categories relative to the references were combined on (c) and (d).
885
886

887 Figure 1

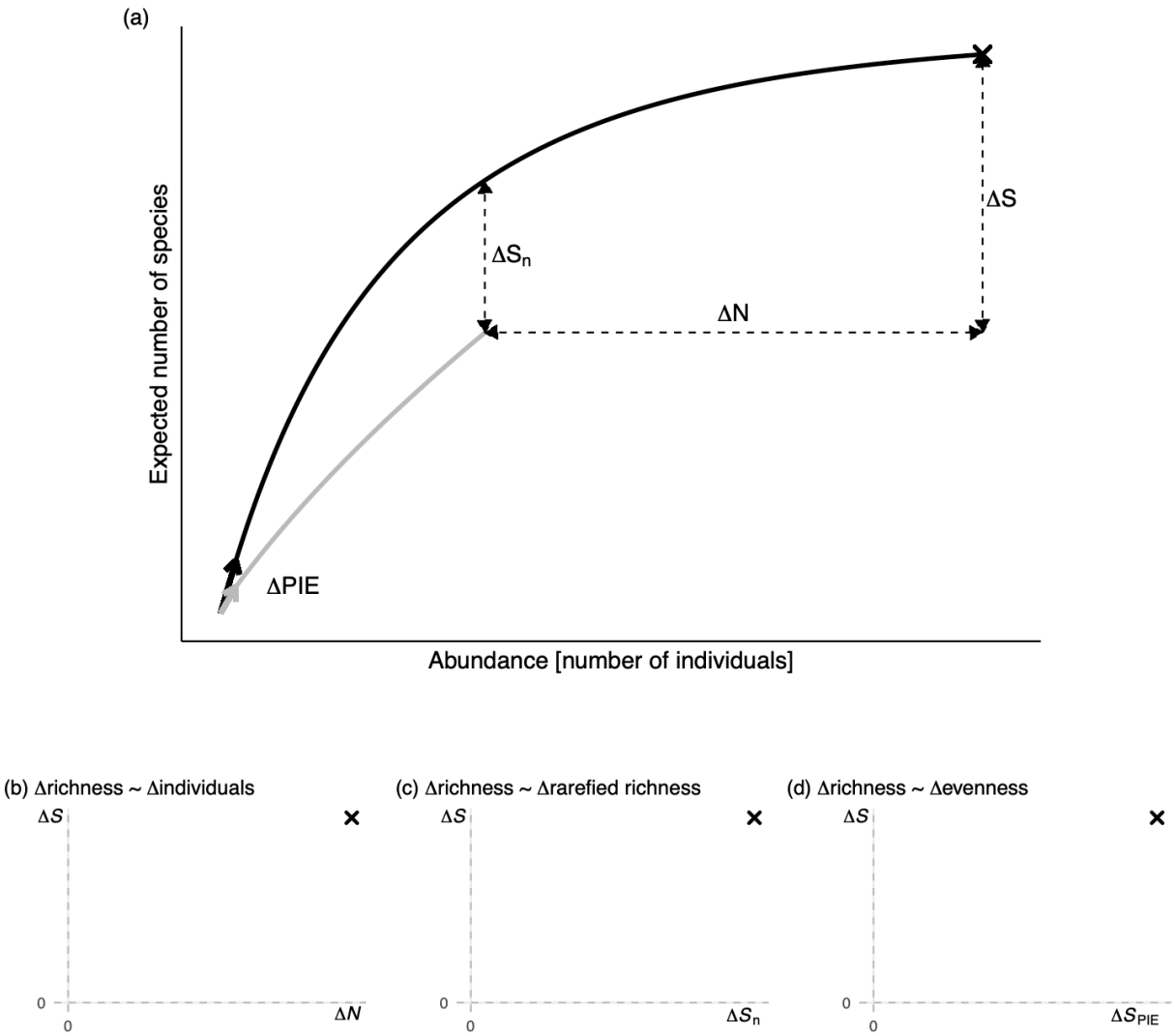

888

Figure 2

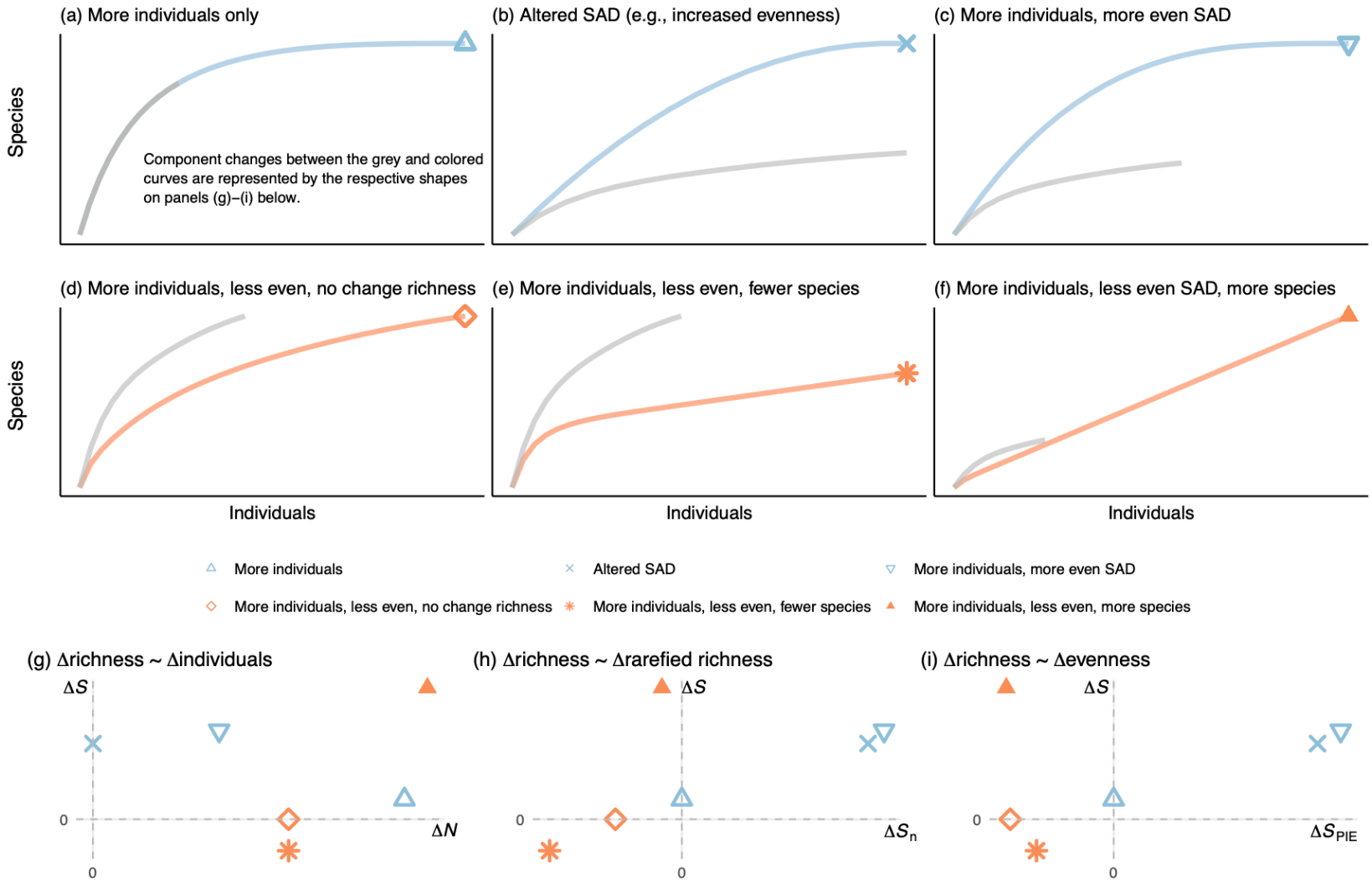
(a) More individuals only
(b) Altered SAD (e.g., increased evenness)
(c) More individuals, more even SAD
Species
Component changes between the grey and colored curves are represented by the respective shapes on panels (g)–(i) below.
(d) More individuals, less even, no change richness
(e) More individuals, less even, fewer species
(f) More individuals, less even SAD, more species
Species
Individuals
Individuals
Individuals
More individuals
Altered SAD
More individuals, more even SAD
More individuals, less even, no change richness
More individuals, less even, fewer species
More individuals, less even, more species
(g) Δrichness ~ Δindividuals
(h) Δrichness ~ Δrarefied richness
(i) Δrichness ~ Δevenness
ΔS
ΔN
ΔS
ΔSn
ΔS
ΔSPIE
0
0
0
0
0
0

Figure 3

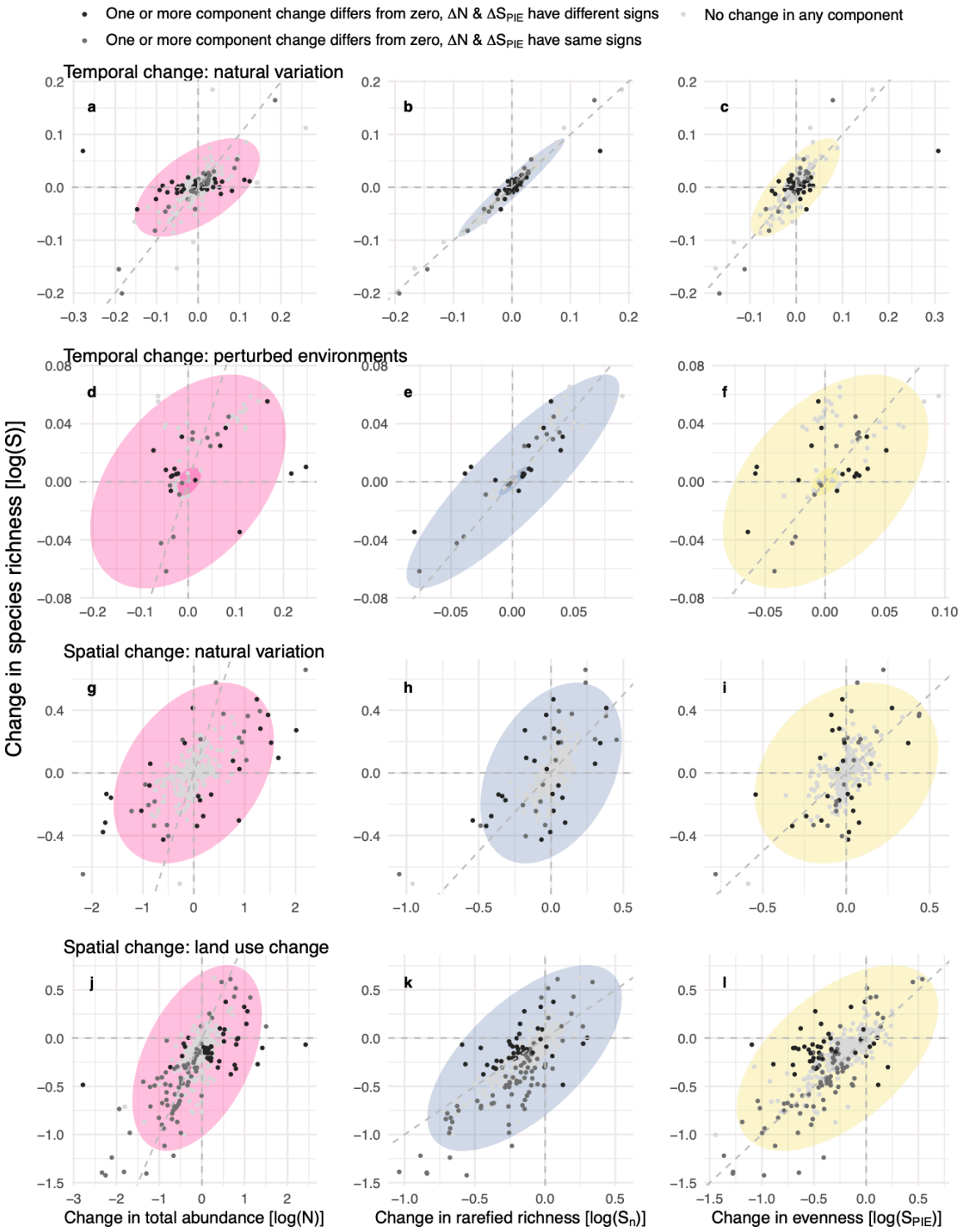
One or more component change differs from zero, ΔN & ΔS_PIE have different signs
No change in any component
One or more component change differs from zero, ΔN & ΔS_PIE have same signs
Temporal change: natural variation
Temporal change: perturbed environments
Spatial change: natural variation
Spatial change: land use change
Change in species richness [log(S)]
Change in total abundance [log(N)]
Change in rarefied richness [log(S_n)]
Change in evenness [log(S_PIE)]

Figure 4

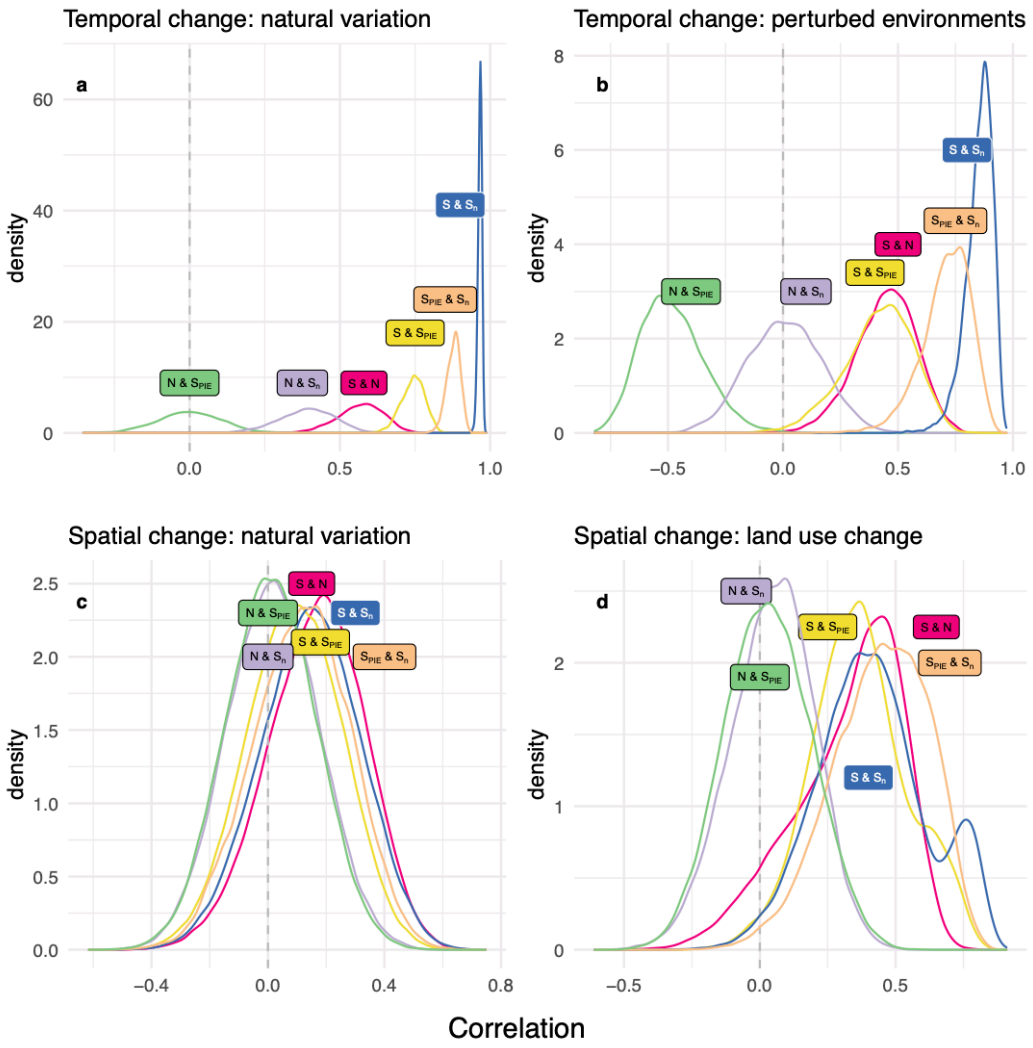
Temporal change: natural variation
a
density
S & Sn
SPIE & Sn
S & SPIE
N & SPIE
N & Sn
S & N
Temporal change: perturbed environments
b
Spatial change: natural variation
c
Spatial change: land use change
d
Correlation

Appendix S1

Title: Local biodiversity change reflects interactions among changing abundance, evenness and richness

Authors: Shane A. Blowes, Gergana N. Daskalova, Maria Dornelas, Thore Engel, Nicholas J. Gotelli, Anne E. Magurran, Inês S. Martins, Brian McGill, Daniel J. McGlinn, Alban Sagouis Hideyasu Shimadzu, Sarah R. Supp, Jonathan M. Chase

Journal: Ecology

Table S1: Countervailing changes in abundance (ΔN) and evenness (ΔS_{PIE}) often result in components other than richness changing. Component(s) with high probability of change as per Figure 2 (i.e., 90% CI does not overlap zero); each row shows the number of assemblages with either countervailing [sign(ΔN) x sign(ΔS_{PIE}) = -1] or abundance and evenness changes with the same direction [sign(ΔN) x sign(ΔS_{PIE}) = 1] for the different data sources.

		Temporal change: natural variation	**Temporal change: perturbed environments**	**Spatial change: natural variation**	**Spatial change: land use change**
Component with high probability of change	sign(ΔN) x sign(ΔS_{PIE})	Number of assemblages	Number of assemblages	Number of assemblages	Number of assemblages
None	-1	97	23	154	107
None	1	131	12	214	191
N only	-1	7	0	7	5
N only	1	2	1	3	5
S_{PIE} only	-1	6	0	1	10
S_{PIE} only	1	2	0	2	12
S_n only	-1	0	1	7	1
S_n only	1	1	1	3	0
S only	-1	1	0	2	1
S only	1	1	0	5	6
S & S_n	-1	0	0	1	1

S & S_n	1	6	2	3	6
S & S_{PIE}	-1	0	0	0	0
S & S_{PIE}	1	1	0	1	3
S & N	-1	1	3	0	3
S & N	1	0	1	3	10
S_n & S_{PIE}	-1	3	4	2	9
S_n & S_{PIE}	1	0	0	0	1
S_n & N	-1	0	0	1	1
S_n & N	1	0	1	0	0
N & S_{PIE}	-1	4	0	0	3
N & S_{PIE}	1	0	0	0	0
S_n, N & S_{PIE}	-1	3	4	0	6
S_n, N & S_{PIE}	1	0	0	0	0
S, N & S_{PIE}	-1	2	0	0	0
S, N & S_{PIE}	1	1	0	0	4
S, S_n, N & S_{PIE}	-1	7	4	0	2
S, S_n, N & S_{PIE}	1	12	6	1	31

Temporal comparisons: natural environmental variation

We fit a model that assumed a lognormal distribution for total abundance (N), and poisson distributions (with log link functions) for species richness (S), rarefied richness (S_n) and evenness (S_{PIE}). We ran the model with four chains for 2000 iterations, with 1000 used as warmup. The model took the following form:

$$N_{ijt} \sim lognormal(\mu_{ijt}^{N}, \sigma),$$

$$S_{ijt} \sim pois(\lambda_{ijt}^{S}),$$

$$S_{n_{ijt}} \sim pois(\lambda_{ijt}^{S_n}),$$

$$S_{PIE_{ijt}} \sim pois(\lambda_{ijt}^{S_{PIE}}),$$

$$\mu_{ijt}^{N} = \beta_0^N + \beta_{0i}^N + \beta_{0ij}^N + (\beta_1^N + \beta_{1i}^N + \beta_{1ij}^N) year_{ijt},$$

$$\log(\lambda_{ijt}^{S}) = \beta_0^S + \beta_{0i}^S + \beta_{0ij}^S + (\beta_1^S + \beta_{1i}^S + \beta_{1ij}^S) year_{ijt},$$

$$\log(\lambda_{ijt}^{S_n}) = \beta_0^{S_n} + \beta_{0i}^{S_n} + \beta_{0ij}^{S_n} + (\beta_1^{S_n} + \beta_{1i}^{S_n} + \beta_{1ij}^{S_n}) year_{ijt},$$

$$\log(\lambda_{ijt}^{S_{PIE}}) = \beta_0^{S_{PIE}} + \beta_{0i}^{S_{PIE}} + \beta_{0ij}^{S_{PIE}} + (\beta_1^{S_{PIE}} + \beta_{1i}^{S_{PIE}} + \beta_{1ij}^{S_{PIE}}) year_{ijt},$$

$$[\beta_{0i}^N, \beta_{0i}^S, \beta_{0i}^{S_n}, \beta_{0i}^{S_{PIE}}, \beta_{1i}^N, \beta_{1i}^S, \beta_{1i}^{S_n}, \beta_{1i}^{S_{PIE}}]' \sim MVNormal(\mathbf{0}, \boldsymbol{SRS}),$$

$$\boldsymbol{S} = \begin{bmatrix} \sigma_{0i}^N & 0 & 0 & 0 & 0 & 0 & 0 & 0 \\ 0 & \sigma_{0i}^S & 0 & 0 & 0 & 0 & 0 & 0 \\ 0 & 0 & \sigma_{0i}^{S_n} & 0 & 0 & 0 & 0 & 0 \\ 0 & 0 & 0 & \sigma_{0i}^{S_{PIE}} & 0 & 0 & 0 & 0 \\ 0 & 0 & 0 & 0 & \sigma_{1i}^N & 0 & 0 & 0 \\ 0 & 0 & 0 & 0 & 0 & \sigma_{1i}^S & 0 & 0 \\ 0 & 0 & 0 & 0 & 0 & 0 & \sigma_{1i}^{S_n} & 0 \\ 0 & 0 & 0 & 0 & 0 & 0 & 0 & \sigma_{1i}^{S_{PIE}} \end{bmatrix},$$

$$\boldsymbol{R} = \begin{bmatrix} 1 & \rho_{N_{0i}S_{0i}} & \rho_{N_{0i}S_{n0i}} & \rho_{N_{0i}S_{PIE0i}} & \rho_{N_{0i}N_{1i}} & \rho_{N_{0i}S_{1i}} & \rho_{N_{0i}S_{n1i}} & \rho_{N_{0i}S_{PIE1i}} \\ \rho_{N_{0i}S_{0i}} & 1 & \rho_{S_{0i}S_{n0i}} & \rho_{S_{0i}S_{PIE0i}} & \rho_{S_{0i}N_{1i}} & \rho_{S_{0i}S_{1i}} & \rho_{S_{0i}S_{n1i}} & \rho_{S_{0i}S_{PIE1i}} \\ \rho_{N_{0i}S_{n0i}} & \rho_{S_{0i}S_{n0i}} & 1 & \rho_{S_{n0i}S_{PIE0i}} & \rho_{S_{n0i}N_{1i}} & \rho_{S_{n0i}S_{1i}} & \rho_{S_{n0i}S_{n1i}} & \rho_{S_{n0i}S_{PIE1i}} \\ \rho_{N_{0i}S_{PIE0i}} & \rho_{S_{0i}S_{PIE0i}} & \rho_{S_{n0i}S_{PIE0i}} & 1 & \rho_{S_{PIE0i}N_{1i}} & \rho_{S_{PIE0i}S_{1i}} & \rho_{S_{PIE0i}S_{n1i}} & \rho_{S_{PIE0i}S_{PIE1i}} \\ \rho_{N_{0i}N_{1i}} & \rho_{S_{0i}N_{1i}} & \rho_{S_{n0i}N_{1i}} & \rho_{S_{PIE0i}N_{1i}} & 1 & \rho_{N_{1i}S_{1i}} & \rho_{N_{1i}S_{n1i}} & \rho_{N_{1i}S_{PIE1i}} \\ \rho_{N_{0i}S_{1i}} & \rho_{S_{0i}S_{1i}} & \rho_{S_{n0i}S_{1i}} & \rho_{S_{PIE0i}S_{1i}} & \rho_{N_{1i}S_{1i}} & 1 & \rho_{S_{1i}S_{n1i}} & \rho_{S_{1i}S_{PIE1i}} \\ \rho_{N_{0i}S_{n1i}} & \rho_{S_{0i}S_{n1i}} & \rho_{S_{n0i}S_{n1i}} & \rho_{S_{PIE0i}S_{n1i}} & \rho_{N_{1i}S_{n1i}} & \rho_{S_{1i}S_{n1i}} & 1 & \rho_{S_{n1i}S_{PIE1i}} \\ \rho_{N_{0i}S_{PIE1i}} & \rho_{S_{0i}S_{PIE1i}} & \rho_{S_{n0i}S_{PIE1i}} & \rho_{S_{PIE0i}S_{PIE1i}} & \rho_{N_{1i}S_{PIE1i}} & \rho_{S_{1i}S_{PIE1i}} & \rho_{S_{n1i}S_{PIE1i}} & 1 \end{bmatrix},$$

$$[\beta_{0ij}^N, \beta_{0ij}^S, \beta_{0ij}^{S_n}, \beta_{0ij}^{S_{PIE}}, \beta_{1ij}^N, \beta_{1ij}^S, \beta_{1ij}^{S_n}, \beta_{1ij}^{S_{PIE}}]' \sim MVNormal(\mathbf{0}, \boldsymbol{SRS}),$$

$$\boldsymbol{S} = \begin{bmatrix} \sigma_{0ij}^{N} & 0 & 0 & 0 & 0 & 0 & 0 & 0 \\ 0 & \sigma_{0ij}^{S} & 0 & 0 & 0 & 0 & 0 & 0 \\ 0 & 0 & \sigma_{0ij}^{S_n} & 0 & 0 & 0 & 0 & 0 \\ 0 & 0 & 0 & \sigma_{0ij}^{S_{PIE}} & 0 & 0 & 0 & 0 \\ 0 & 0 & 0 & 0 & \sigma_{1ij}^{N} & 0 & 0 & 0 \\ 0 & 0 & 0 & 0 & 0 & \sigma_{1ij}^{S} & 0 & 0 \\ 0 & 0 & 0 & 0 & 0 & 0 & \sigma_{1ij}^{S_n} & 0 \\ 0 & 0 & 0 & 0 & 0 & 0 & 0 & \sigma_{1ij}^{S_{PIE}} \end{bmatrix},$$

$$R = \begin{bmatrix} 1 & \rho_{N_{0ij}S_{0ij}} & \rho_{N_{0ij}S_{n_{0ij}}} & \rho_{N_{0ij}S_{PIE_{0ij}}} & \rho_{N_{0ij}N_{1ij}} & \rho_{N_{0ij}S_{1ij}} & \rho_{N_{0ij}S_{n_{1ij}}} & \rho_{N_{0ij}S_{PIE_{1ij}}} \\ \rho_{N_{0ij}S_{0ij}} & 1 & \rho_{S_{0ij}S_{n_{0ij}}} & \rho_{S_{0ij}S_{PIE_{0ij}}} & \rho_{S_{0ij}N_{1ij}} & \rho_{S_{0ij}S_{1ij}} & \rho_{S_{0ij}S_{n_{1ij}}} & \rho_{S_{0ij}S_{PIE_{1ij}}} \\ \rho_{N_{0ij}S_{n_{0ij}}} & \rho_{S_{0ij}S_{n_{0ij}}} & 1 & \rho_{S_{n_{0ij}}S_{PIE_{0ij}}} & \rho_{S_{n_{0ij}}N_{1ij}} & \rho_{S_{n_{0ij}}S_{1ij}} & \rho_{S_{n_{0ij}}S_{n_{1ij}}} & \rho_{S_{n_{0ij}}S_{PIE_{1ij}}} \\ \rho_{N_{0ij}S_{PIE_{0ij}}} & \rho_{S_{0ij}S_{PIE_{0ij}}} & \rho_{S_{n_{0ij}}S_{PIE_{0ij}}} & 1 & \rho_{S_{PIE_{0ij}}N_{1ij}} & \rho_{S_{PIE_{0ij}}S_{1ij}} & \rho_{S_{PIE_{0ij}}S_{n_{1ij}}} & \rho_{S_{PIE_{0ij}}S_{PIE_{1ij}}} \\ \rho_{N_{0ij}N_{1ij}} & \rho_{S_{0ij}N_{1ij}} & \rho_{S_{n_{0ij}}N_{1ij}} & \rho_{S_{PIE_{0ij}}N_{1ij}} & 1 & \rho_{N_{1ij}S_{1ij}} & \rho_{N_{1ij}S_{n_{1ij}}} & \rho_{N_{1ij}S_{PIE_{1ij}}} \\ \rho_{N_{0ij}S_{1ij}} & \rho_{S_{0ij}S_{1ij}} & \rho_{S_{n_{0ij}}S_{1ij}} & \rho_{S_{PIE_{0ij}}S_{1ij}} & \rho_{N_{1ij}S_{1ij}} & 1 & \rho_{S_{1ij}S_{n_{1ij}}} & \rho_{S_{1ij}S_{PIE_{1ij}}} \\ \rho_{N_{0ij}S_{n_{1ij}}} & \rho_{S_{0ij}S_{n_{1ij}}} & \rho_{S_{n_{0ij}}S_{n_{1ij}}} & \rho_{S_{PIE_{0ij}}S_{n_{1ij}}} & \rho_{N_{1ij}S_{n_{1ij}}} & \rho_{S_{1ij}S_{n_{1ij}}} & 1 & \rho_{S_{n_{1ij}}S_{PIE_{1ij}}} \\ \rho_{N_{0ij}S_{PIE_{1ij}}} & \rho_{S_{0ij}S_{PIE_{1ij}}} & \rho_{S_{n_{0ij}}S_{PIE_{1ij}}} & \rho_{S_{PIE_{0ij}}S_{PIE_{1ij}}} & \rho_{N_{1ij}S_{PIE_{1ij}}} & \rho_{S_{1ij}S_{PIE_{1ij}}} & \rho_{S_{n_{1ij}}S_{PIE_{1ij}}} & 1 \end{bmatrix},$$

$$\beta_0^N, \beta_0^S, \beta_0^{S_n}, \beta_0^{S_{PIE}} \sim N(0,1),$$

$$\beta_1^N, \beta_1^S, \beta_1^{S_n}, \beta_1^{S_{PIE}} \sim N(0,0.2),$$

$$\sigma_{0i}^S, \sigma_{0i}^{S_n}, \sigma_{0i}^{S_{PIE}}, \sigma_{1i}^S, \sigma_{1i}^{S_n}, \sigma_{1i}^{S_{PIE}}, \sigma_{0ij}^S, \sigma_{0ij}^{S_n}, \sigma_{0ij}^{S_{PIE}}, \sigma_{1ij}^S, \sigma_{1ij}^{S_n}, \sigma_{1ij}^{S_{PIE}} \sim student(3,0,10),$$

$$\sigma, \sigma_{0i}^N, \sigma_{1ij}^N, \sigma_{0ij}^N, \sigma_{1ij}^N \sim student(3,0,16),$$

$$\boldsymbol{R} \sim LJK(1),$$

where N_{ijt}, S_{ijt}, $S_{n_{ijt}}$, and $S_{PIE_{ijt}}$ are the values of each of the metrics in the *j*th cell of the *i*th study in year *t*, and $year_{ijt}$ is the time in years. β_0 and β_1 (with the respective superscripts for each metric) represent the non-varying intercepts and slopes, respectively. β_{0i} and β_{1i} (with the respective superscripts for each metric) represent the varying intercepts and slopes for study-level departures from β_0 and β_1, respectively. β_{0ij} and β_{1ij} (with the respective superscripts for each metric) represent the varying intercepts and slopes for cell-level departures from β_0 and β_1, respectively. The covariance matrices of each multivariate normal distribution for varying effects (one each for the study- and cell-level departures) are parameterised in terms of a correlation matrix **R** and two matrices **S** with diagonal elements σ (superscripts for metrics, subscripts denote intercept (0), slopes (1) and level: studies *i* and cells *j*).

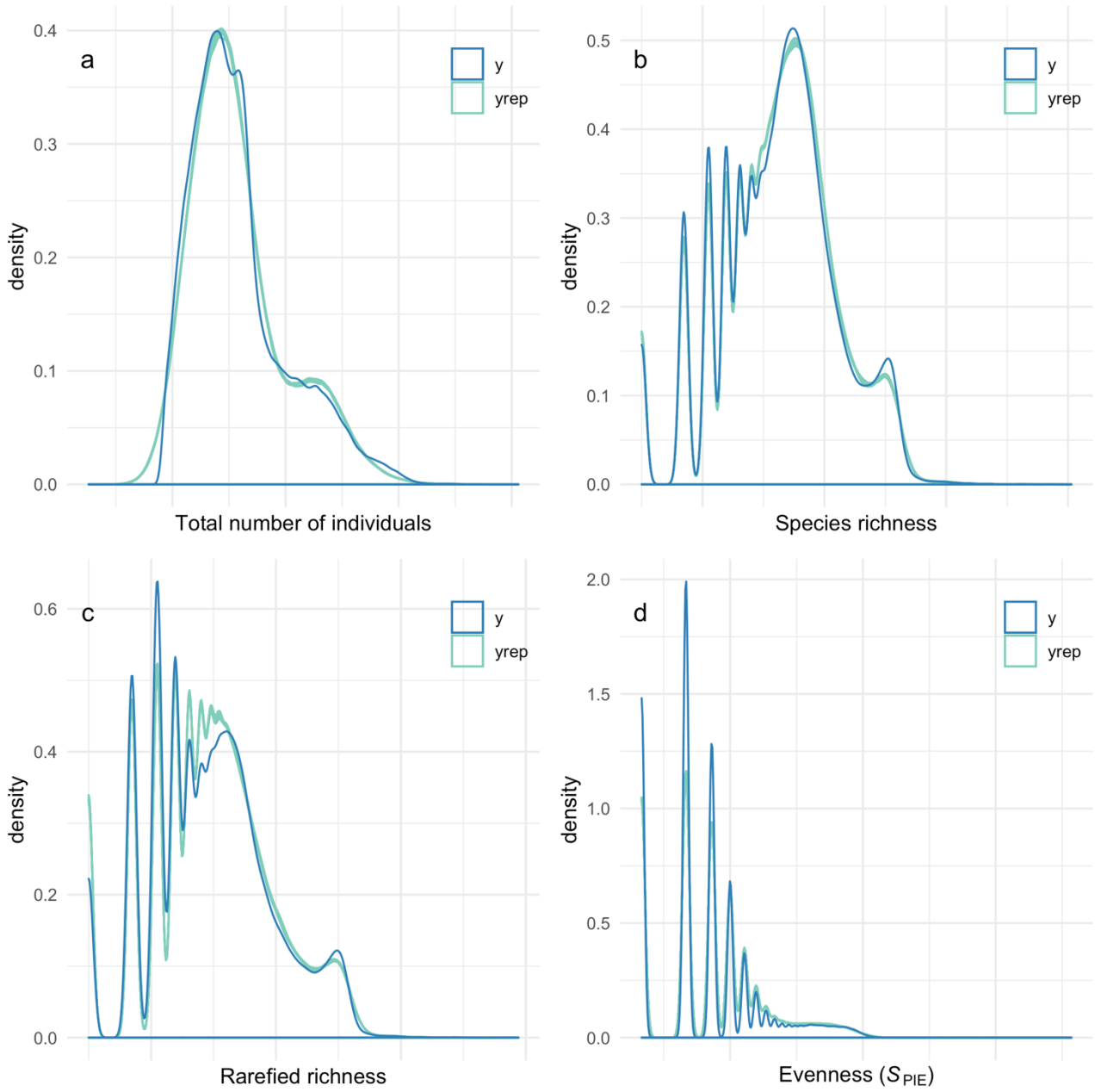

Figure S1: Posterior predictive checks for the model fit to the temporal data in naturally varying environments. (a) Total numbers of individuals, (b) species richness, (c) rarefied richness (S_n) and (d) evenness (S_{PIE}). Each panel shows the density of the data (y) and ten draws of the posterior distribution (yrep).

Temporal comparisons: experimental or natural perturbations

We fit a model that assumed lognormal distributions for all response variables (N, S, S_n, S_{PIE}). Our focus is on the treatment-level variation in the metrics, and we created a covariate that was the concatenation of study and treatment to this end. Additionally, as some studies had blocks within sites, and others did not, we created a new variable that was the concatenation of site and block, where those without block had no unique identifier. We ran the model with four chains for 3000 iterations, with 1500 used as warmup. The model took the following form:

$$N_{ijkt} \sim lognormal\left(\mu^{N}_{ijkt}, \sigma^{N}\right),$$

$$S_{ijkt} \sim lognormal\left(\mu^{S}_{ijkt}, \sigma^{S}\right),$$

$$S_{n\,ijkt} \sim lognormal\left(\mu^{S_n}_{ijkt}, \sigma^{S_n}\right),$$

$$S_{PIE\,ijkt} \sim lognormal\left(\mu^{S_{PIE}}_{ijkt}, \sigma^{S_{PIE}}\right),$$

$$\mu^{N}_{ijkt} = \beta^{N}_{0} + \beta^{N}_{0i} + \beta^{N}_{0j} + \beta^{N}_{0k} + (\beta^{N}_{1} + \beta^{N}_{1k})year_{ijkt},$$

$$\mu^{S}_{ijkt} = \beta^{S}_{0} + \beta^{S}_{0i} + \beta^{S}_{0j} + \beta^{S}_{0k} + (\beta^{S}_{1} + \beta^{S}_{1k})year_{ijkt},$$

$$\mu^{S_n}_{ijkt} = \beta^{S_n}_{0} + \beta^{S_n}_{0i} + \beta^{S_n}_{0j} + \beta^{S_n}_{0k} + (\beta^{S_n}_{1} + \beta^{S_n}_{1k})year_{ijkt},$$

$$\mu^{S_{PIE}}_{ijkt} = \beta^{S_{PIE}}_{0} + \beta^{S_{PIE}}_{0i} + \beta^{S_{PIE}}_{0j} + \beta^{S_{PIE}}_{0k} + \left(\beta^{S_{PIE}}_{1} + \beta^{S_{PIE}}_{1k}\right)year_{ijkt},$$

$$\left[\beta^{N}_{0k}, \beta^{S}_{0k}, \beta^{S_n}_{0k}, \beta^{S_{PIE}}_{0k}, \beta^{N}_{1k}, \beta^{S}_{1k}, \beta^{S_n}_{1k}, \beta^{S_{PIE}}_{1k}\right]' \sim MVNormal(\mathbf{0}, \boldsymbol{SRS}),$$

$$\boldsymbol{S} = \begin{bmatrix} \sigma^{N}_{0k} & 0 & 0 & 0 & 0 & 0 & 0 & 0 \\ 0 & \sigma^{S}_{0k} & 0 & 0 & 0 & 0 & 0 & 0 \\ 0 & 0 & \sigma^{S_n}_{0k} & 0 & 0 & 0 & 0 & 0 \\ 0 & 0 & 0 & \sigma^{S_{PIE}}_{0k} & 0 & 0 & 0 & 0 \\ 0 & 0 & 0 & 0 & \sigma^{N}_{1k} & 0 & 0 & 0 \\ 0 & 0 & 0 & 0 & 0 & \sigma^{S}_{1k} & 0 & 0 \\ 0 & 0 & 0 & 0 & 0 & 0 & \sigma^{S_n}_{1k} & 0 \\ 0 & 0 & 0 & 0 & 0 & 0 & 0 & \sigma^{S_{PIE}}_{1k} \end{bmatrix},$$

$$\boldsymbol{R} = \begin{bmatrix} 1 & \rho_{N_{0k}S_{0k}} & \rho_{N_{0k}S_{n0k}} & \rho_{N_{0k}S_{PIE_{0k}}} & \rho_{N_{0k}N_{1k}} & \rho_{N_{0k}S_{1k}} & \rho_{N_{0k}S_{n1k}} & \rho_{N_{0k}S_{PIE_{1k}}} \\ \rho_{N_{0k}S_{0k}} & 1 & \rho_{S_{0k}S_{n0k}} & \rho_{S_{0k}S_{PIE_{0k}}} & \rho_{S_{0k}N_{1k}} & \rho_{S_{0k}S_{1k}} & \rho_{S_{0k}S_{n1k}} & \rho_{S_{0k}S_{PIE_{1k}}} \\ \rho_{N_{0k}S_{n0k}} & \rho_{S_{0k}S_{n0k}} & 1 & \rho_{S_{n0k}S_{PIE_{0k}}} & \rho_{S_{n0k}N_{1k}} & \rho_{S_{n0k}S_{1k}} & \rho_{S_{n0k}S_{n1k}} & \rho_{S_{n0k}S_{PIE_{1k}}} \\ \rho_{N_{0k}S_{PIE_{0k}}} & \rho_{S_{0k}S_{PIE_{0k}}} & \rho_{S_{n0k}S_{PIE_{0k}}} & 1 & \rho_{S_{PIE_{0k}}N_{1k}} & \rho_{S_{PIE_{0k}}S_{1k}} & \rho_{S_{PIE_{0k}}S_{n1k}} & \rho_{S_{PIE_{0k}}S_{PIE_{1k}}} \\ \rho_{N_{0k}N_{1k}} & \rho_{S_{0k}N_{1k}} & \rho_{S_{n0k}N_{1k}} & \rho_{S_{PIE_{0k}}N_{1k}} & 1 & \rho_{N_{1k}S_{1k}} & \rho_{N_{1k}S_{n1k}} & \rho_{N_{1k}S_{PIE_{1k}}} \\ \rho_{N_{0k}S_{1k}} & \rho_{S_{0k}S_{1k}} & \rho_{S_{n0k}S_{1k}} & \rho_{S_{PIE_{0k}}S_{1k}} & \rho_{N_{1k}S_{1k}} & 1 & \rho_{S_{1k}S_{n1k}} & \rho_{S_{1k}S_{PIE_{1k}}} \\ \rho_{N_{0k}S_{n1k}} & \rho_{S_{0k}S_{n1k}} & \rho_{S_{n0k}S_{n1k}} & \rho_{S_{PIE_{0k}}S_{n1k}} & \rho_{N_{1k}S_{n1k}} & \rho_{S_{1k}S_{n1k}} & 1 & \rho_{S_{n1k}S_{PIE_{1k}}} \\ \rho_{N_{0k}S_{PIE_{1k}}} & \rho_{S_{0k}S_{PIE_{1k}}} & \rho_{S_{n0k}S_{PIE_{1i}}} & \rho_{S_{PIE_{0k}}S_{PIE_{1k}}} & \rho_{N_{1k}S_{PIE_{1k}}} & \rho_{S_{1k}S_{PIE_{1k}}} & \rho_{S_{n1k}S_{PIE_{1k}}} & 1 \end{bmatrix},$$

$$\beta^{N}_{0}, \beta^{S}_{0}, \beta^{S_n}_{0}, \beta^{S_{PIE}}_{0} \sim N(0, 1),$$

$$\beta^{N}_{1}, \beta^{S}_{1}, \beta^{S_n}_{1}, \beta^{S_{PIE}}_{1} \sim N(0, 0.2),$$

$$\sigma^{S}_{0i}, \sigma^{S_n}_{0i}, \sigma^{S_{PIE}}_{0i}, \sigma^{S}_{1i}, \sigma^{S_n}_{1i}, \sigma^{S_{PIE}}_{1i}, \sigma^{S}_{0ij}, \sigma^{S_n}_{0ij}, \sigma^{S_{PIE}}_{0ij}, \sigma^{S}_{1ij}, \sigma^{S_n}_{1ij}, \sigma^{S_{PIE}}_{1ij} \sim normal(0, 1),$$

$$\sigma, \sigma^{N}_{0i}, \sigma^{N}_{1ij}, \sigma^{N}_{0ij}, \sigma^{N}_{1ij} \sim student(3, 0, 16),$$

$$\boldsymbol{R} \sim LJK(1),$$

where N_{ijkt}, S_{ijkt}, $S_{n_{ijkt}}$, and $S_{PIE_{ijkt}}$ are the values of each of the metrics in the kth study-treatment combination, for the *j*th study-block combination of the *i*th study in year *t*, and $year_{ijkt}$ is the time in years. β_0 and β_1 (with the respective superscripts for each metric) represent the non-varying intercepts and slopes, respectively. β_{0i} (with the respective superscripts for each metric) represent the varying intercepts study-level departures from β_0, and β_{0j} (with the respective superscripts for each metric) represent the varying intercepts study-block level departures from β_0. β_{0k} and β_{1k} (with the respective superscripts for each metric) represent the varying intercepts and slopes for study-treatment departures from β_0 and β_1, respectively. The covariance matrix of the multivariate normal distribution for varying study-treatment effects were parameterised in terms of a correlation matrix **R** and two matrices **S** with diagonal elements σ (superscripts for metrics, subscripts denote intercept (0), slopes (1) and study-treatment combination, *k*).

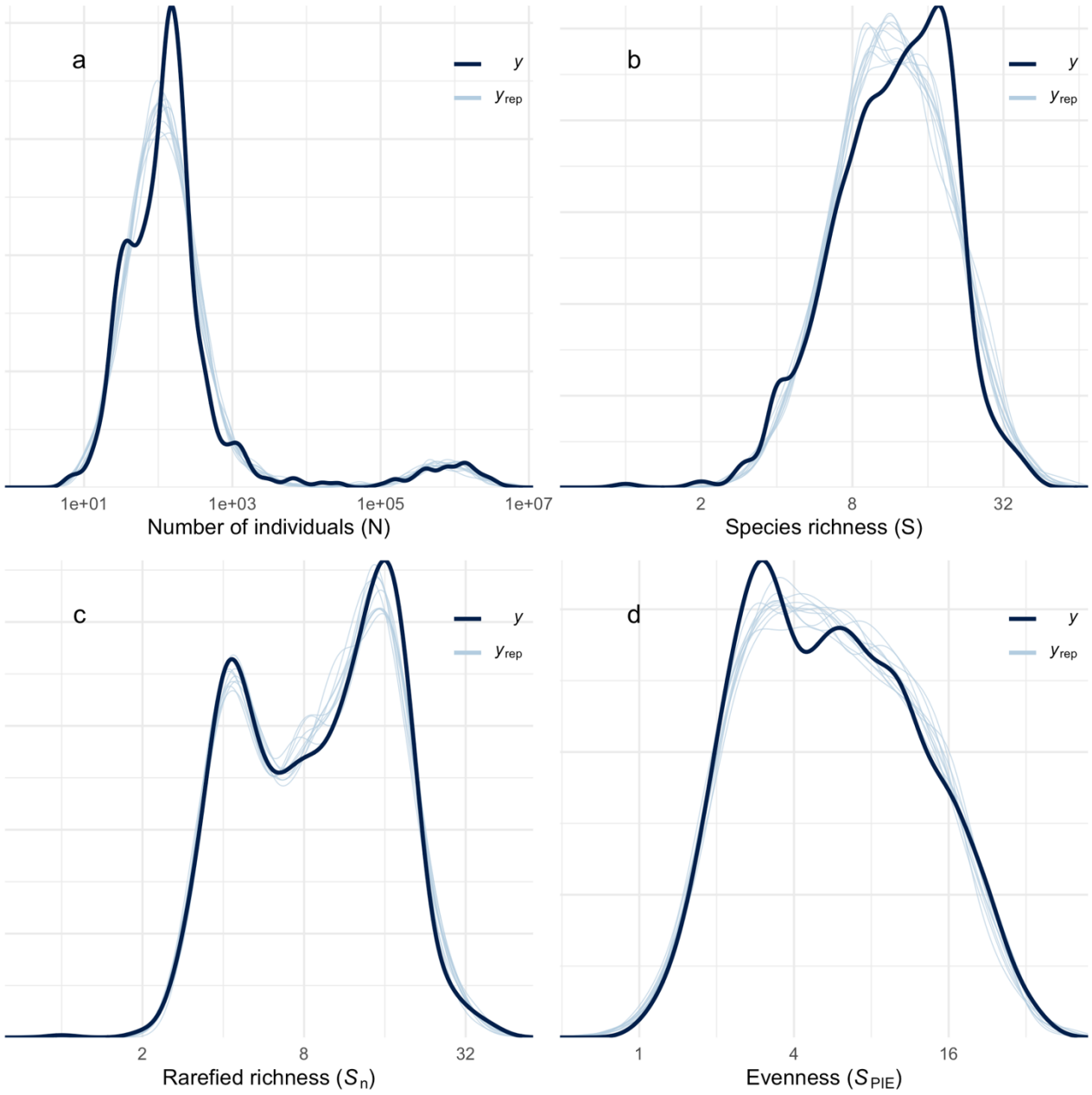

Figure S2: Posterior predictive checks for the model fit to the temporal data in perturbed environments. (a) Total numbers of individuals, (b) species richness, (c) rarefied richness (Sn) and (d) evenness (SPIE).). Each panel shows the density of the data (y) and ten draws of the posterior distribution (yrep).

References (for times series with experimental or natural perturbations)

Bateman, H., D. Childers, and P. Warren. 2018. Point-count bird censusing: long-term monitoring of bird abundance and diversity along the Salt River in the greater Phoenix metropolitan area, ongoing since 2013 ver 3.

Carpenter, S., J. Kitchell, J. Cole, and M. Pace. 2017. Cascade Project at North Temperate Lakes LTER Core Data Zooplankton 1984 - 2016 ver 4. Environmental Data Initiative.

Carpenter, S., J. Kitchell, J. Cole, and M. Pace. 2017. Cascade Project at North Temperate Lakes LTER Core Data Phytoplankton 1984 - 2015 ver 4. Environmental Data Initiative.

Ellison, A. and R. Dunn. 2018. Ants Under Climate Change at Harvard Forest and Duke Forest 2009-2015 ver 57. Environmental Data Initiative.

Philip Grime and Jason Fridley. Point Quadrat Vegetation Data, Buxton Climate Change Experiment, UK, 1994-2009. Knowledge Network for Biocomplexity. doi:10.5063/AA/fridley.3.2.

Hershey, A. 2016. Total numbers and species of insects taken from rock scrubbings during the summer of 1984-1988, 1993-1994, 1996-1998, in the Kuparuk River experimental reach near Toolik Field Station, North Slope Alaska.. ver 3. Environmental Data Initiative.

Joern, A. 2020. CGR02 Sweep Sampling of Grasshoppers on Konza Prairie LTER watersheds ver 14. Environmental Data Initiative.

Joern, A. 2020. PBG07 Grasshopper species abundances in the Patch-Burn Grazing experiment at Konza Prairie ver 5. Environmental Data Initiative.

Knops, J. 2018. Arthropod sweep net sampling: Interactive Effects of Deer, Fire and Nitrogen ver 8. Environmental Data Initiative.

Knops, J. 2018. Small mammal abundance: Interactive Effects of Deer, Fire and Nitrogen ver 8. Environmental Data Initiative.

Santa Barbara Coastal LTER and D. Reed. 2020. SBC LTER: Reef: Long-term experiment: Kelp removal: Fish abundance ver 18. Environmental Data Initiative.

Spatial comparisons: natural environmental variation

We fit a model that assumed lognormal distributions for N, S_n, and S_{PIE}, and a Poisson distribution (and log link function) for S. We fit the model with four chains and 4000 iterations, with 2000 as warmup. The model took the following form:

$$N_{ij} \sim lognormal(\mu_{ij}^{N}, \sigma^{N}),$$

$$S_{ij} \sim poisson(\lambda_{ij}^{S}),$$

$$S_{n_{ij}} \sim lognormal(\mu_{ij}^{S_n}, \sigma^{S_n}),$$

$$S_{PIE_{ij}} \sim lognormal(\mu_{ij}^{S_{PIE}}, \sigma^{S_{PIE}}), \quad \text{(S1.4)}$$

$$\mu_{ij}^{N} = \beta_0^{N} + \beta_{0j}^{N} + (\beta_{1j}^{N}) site_{ij},$$

$$\log(\lambda_{ij}^{S}) = \beta_0^{S} + \beta_{0i}^{S} + \beta_{0j}^{S} + (\beta_{1j}^{S}) site_{ij},$$

$$\mu_{ij}^{S_n} = \beta_0^{S_n} + \beta_{0j}^{S_n} + (\beta_{1j}^{S_n}) site_{ij},$$

$$\mu_{ij}^{S_{PIE}} = \beta_0^{S_{PIE}} + \beta_{0j}^{S_{PIE}} + (\beta_{1j}^{S_{PIE}}) site_{ij},$$

$$\left[\beta_{0j}^{N}, \beta_{0j}^{S}, \beta_{0j}^{S_n}, \beta_{0j}^{S_{PIE}}, \beta_{1j}^{N}, \beta_{1j}^{S}, \beta_{1j}^{S_n}, \beta_{1j}^{S_{PIE}}\right]' \sim MVNormal(\mathbf{0}, \boldsymbol{SRS}),$$

$$\boldsymbol{S} = \begin{bmatrix} \sigma_{0j}^{N} & 0 & 0 & 0 & 0 & 0 & 0 & 0 \\ 0 & \sigma_{0j}^{S} & 0 & 0 & 0 & 0 & 0 & 0 \\ 0 & 0 & \sigma_{0j}^{S_n} & 0 & 0 & 0 & 0 & 0 \\ 0 & 0 & 0 & \sigma_{0j}^{S_{PIE}} & 0 & 0 & 0 & 0 \\ 0 & 0 & 0 & 0 & \sigma_{1j}^{N} & 0 & 0 & 0 \\ 0 & 0 & 0 & 0 & 0 & \sigma_{1j}^{S} & 0 & 0 \\ 0 & 0 & 0 & 0 & 0 & 0 & \sigma_{1j}^{S_n} & 0 \\ 0 & 0 & 0 & 0 & 0 & 0 & 0 & \sigma_{1j}^{S_{PIE}} \end{bmatrix},$$

$$\boldsymbol{R} = \begin{bmatrix} 1 & \rho_{N_{0j}S_{0j}} & \rho_{N_{0j}S_{n_{0j}}} & \rho_{N_{0j}S_{PIE_{0j}}} & \rho_{N_{0j}N_{1j}} & \rho_{N_{0j}S_{1j}} & \rho_{N_{0j}S_{n_{1j}}} & \rho_{N_{0j}S_{PIE_{1j}}} \\ \rho_{N_{0j}S_{0j}} & 1 & \rho_{S_{0j}S_{n_{0j}}} & \rho_{S_{0j}S_{PIE_{0j}}} & \rho_{S_{0j}N_{1j}} & \rho_{S_{0j}S_{1j}} & \rho_{S_{0j}S_{n_{1j}}} & \rho_{S_{0j}S_{PIE_{1j}}} \\ \rho_{N_{0j}S_{n_{0j}}} & \rho_{S_{0j}S_{n_{0j}}} & 1 & \rho_{S_{n_{0j}}S_{PIE_{0j}}} & \rho_{S_{n_{0j}}N_{1j}} & \rho_{S_{n_{0j}}S_{1j}} & \rho_{S_{n_{0j}}S_{n_{1j}}} & \rho_{S_{n_{0j}}S_{PIE_{1j}}} \\ \rho_{N_{0j}S_{PIE_{0j}}} & \rho_{S_{0j}S_{PIE_{0j}}} & \rho_{S_{n_{0j}}S_{PIE_{0j}}} & 1 & \rho_{S_{PIE_{0j}}N_{1j}} & \rho_{S_{PIE_{0j}}S_{1j}} & \rho_{S_{PIE_{0j}}S_{n_{1j}}} & \rho_{S_{PIE_{0j}}S_{PIE_{1j}}} \\ \rho_{N_{0j}N_{1j}} & \rho_{S_{0j}N_{1j}} & \rho_{S_{n_{0j}}N_{1j}} & \rho_{S_{PIE_{0j}}N_{1j}} & 1 & \rho_{N_{1j}S_{1j}} & \rho_{N_{1j}S_{n_{1j}}} & \rho_{N_{1j}S_{PIE_{1j}}} \\ \rho_{N_{0j}S_{1j}} & \rho_{S_{0j}S_{1j}} & \rho_{S_{n_{0j}}S_{1j}} & \rho_{S_{PIE_{0j}}S_{1j}} & \rho_{N_{1j}S_{1j}} & 1 & \rho_{S_{1j}S_{n_{1j}}} & \rho_{S_{1j}S_{PIE_{1j}}} \\ \rho_{N_{0j}S_{n_{1j}}} & \rho_{S_{0j}S_{n_{1j}}} & \rho_{S_{n_{0j}}S_{n_{1j}}} & \rho_{S_{PIE_{0j}}S_{n_{1j}}} & \rho_{N_{1j}S_{n_{1j}}} & \rho_{S_{1j}S_{n_{1j}}} & 1 & \rho_{S_{n_{1j}}S_{PIE_{1j}}} \\ \rho_{N_{0j}S_{PIE_{1j}}} & \rho_{S_{0k}S_{PIE_{1j}}} & \rho_{S_{n_{0j}}S_{PIE_{1j}}} & \rho_{S_{PIE_{0j}}S_{PIE_{1j}}} & \rho_{N_{1j}S_{PIE_{1j}}} & \rho_{S_{1j}S_{PIE_{1j}}} & \rho_{S_{n_{1j}}S_{PIE_{1j}}} & 1 \end{bmatrix},$$

$$\beta_0^{N}, \beta_0^{S}, \beta_0^{S_n}, \beta_0^{S_{PIE}} \sim N(0,1),$$

$$\sigma^{N}, \sigma^{S_n}, \sigma^{S_{PIE}}, \sigma_{0i}^{S}, \sigma_{0j}^{N}, \sigma_{0j}^{S}, \sigma_{0j}^{S_n}, \sigma_{0j}^{S_{PIE}}, \sigma_{1j}^{N}, \sigma_{1j}^{S}, \sigma_{1j}^{S_n}, \sigma_{1j}^{S_{PIE}} \sim normal(0,1),$$

$$\boldsymbol{R} \sim LJK(1),$$

where N_{ij}, S_{ij}, $S_{n_{ij}}$, and $S_{PIE_{ij}}$ are the values of each of the metrics for the ith observation in the jth study-site combination, and $site_{ij}$ is site identifier. β_0 (with the respective superscripts for each metric) represent the non-varying intercepts for each data source (one each for CESTES and

McGill), respectively. β_{0i}^{S} is an observation level varying intercept to model overdispersion in *S*. β_{0j} and β_{1j} (with the respective superscripts for each metric) represent the varying intercepts (reference sites for each study) and slopes (departures for all other sites). The covariance matrix of the multivariate normal distribution for varying study-site effects were parameterised in terms of a correlation matrix **R** and two matrices **S** with diagonal elements σ (superscripts for metrics, subscripts denote intercept (0), slopes (1)).

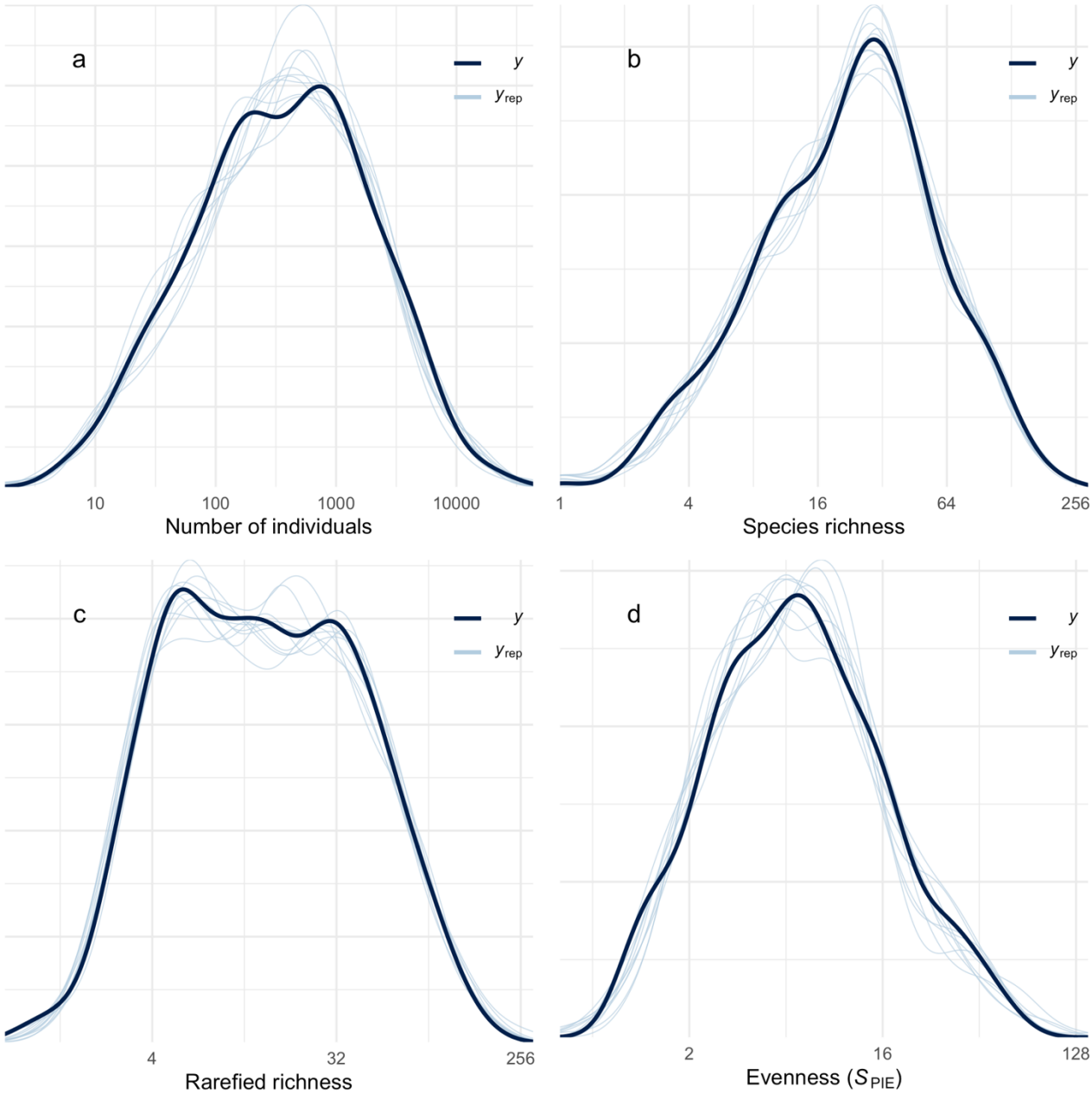

Figure S3: Posterior predictive checks for the model fit to the spatial data in natural environments. (a) Total numbers of individuals, (b) species richness, (c) rarefied richness (S_n) and (d) evenness (S_{PIE}). Each panel shows the density of the data (y) and ten draws of the posterior distribution (yrep).

Spatial comparisons: anthropogenic perturbations

We fit a model that assumed lognormal distributions for N, S_n, and S_{PIE}, and a Poisson distribution (and log link function) for S. We fit the model with four chains and 4000 iterations, with 2000 used as warmup. The model took the following form:

$$N_{ijk} \sim lognormal\left(\mu_{ijk}^{N}, \sigma^{N}\right),$$

$$S_{ijk} \sim poisson\left(\lambda_{ijk}^{S}\right),$$

$$S_{n_{ijk}} \sim lognormal\left(\mu_{ijk}^{S_n}, \sigma^{S_n}\right),$$

$$S_{PIE_{ijk}} \sim lognormal\left(\mu_{ijk}^{S_{PIE}}, \sigma^{S_{PIE}}\right),$$

$$\mu_{ijk}^{N} = \beta_0^N + \beta_{0j}^N + \beta_{0k}^N + (\beta_1^N + \beta_{1k}^N)LU_{ij},$$

$$\log\left(\lambda_{ijk}^{S}\right) = \beta_0^S + \beta_{0i}^S + \beta_{0j}^S + \beta_{0k}^S + (\beta_1^S + \beta_{1k}^S)LU_{ijk},$$

$$\mu_{ijk}^{S_n} = \beta_0^{S_n} + \beta_{0j}^{S_n} + \beta_{0k}^{S_n} + (\beta_1^{S_n} + \beta_{1k}^{S_n})LU_{ijk},$$

$$\mu_{ijk}^{S_{PIE}} = \beta_0^{S_{PIE}} + \beta_{0j}^{S_{PIE}} + \beta_{0k}^{S_{PIE}} + (\beta_1^{S_{PIE}} + \beta_{1k}^{S_{PIE}})LU_{ijk},$$

$$\left[\beta_{0j}^N, \beta_{0j}^S, \beta_{0j}^{S_n}, \beta_{0j}^{S_{PIE}}, \beta_{1j}^N, \beta_{1j}^S, \beta_{1j}^{S_n}, \beta_{1j}^{S_{PIE}}\right]' \sim MVNormal(\mathbf{0}, \boldsymbol{SRS}),$$

$$\boldsymbol{S} = \begin{bmatrix} \sigma_{0k}^N & 0 & 0 & 0 & 0 & 0 & 0 & 0 \\ 0 & \sigma_{0k}^S & 0 & 0 & 0 & 0 & 0 & 0 \\ 0 & 0 & \sigma_{0k}^{S_n} & 0 & 0 & 0 & 0 & 0 \\ 0 & 0 & 0 & \sigma_{0k}^{S_{PIE}} & 0 & 0 & 0 & 0 \\ 0 & 0 & 0 & 0 & \sigma_{1k}^N & 0 & 0 & 0 \\ 0 & 0 & 0 & 0 & 0 & \sigma_{1k}^S & 0 & 0 \\ 0 & 0 & 0 & 0 & 0 & 0 & \sigma_{1k}^{S_n} & 0 \\ 0 & 0 & 0 & 0 & 0 & 0 & 0 & \sigma_{1k}^{S_{PIE}} \end{bmatrix},$$

$$\boldsymbol{R} = \begin{bmatrix} 1 & \rho_{N_{0k}S_{0k}} & \rho_{N_{0k}S_{n_{0k}}} & \rho_{N_{0k}S_{PIE_{0k}}} & \rho_{N_{0k}N_{1k}} & \rho_{N_{0k}S_{1k}} & \rho_{N_{0k}S_{n_{1k}}} & \rho_{N_{0k}S_{PIE_{1k}}} \\ \rho_{N_{0k}S_{0k}} & 1 & \rho_{S_{0k}S_{n_{0k}}} & \rho_{S_{0k}S_{PIE_{0k}}} & \rho_{S_{0k}N_{1k}} & \rho_{S_{0k}S_{1k}} & \rho_{S_{0k}S_{n_{1k}}} & \rho_{S_{0k}S_{PIE_{1k}}} \\ \rho_{N_{0k}S_{n_{0k}}} & \rho_{S_{0k}S_{n_{0k}}} & 1 & \rho_{S_{n_{0k}}S_{PIE_{0k}}} & \rho_{S_{n_{0k}}N_{1k}} & \rho_{S_{n_{0k}}S_{1k}} & \rho_{S_{n_{0k}}S_{n_{1k}}} & \rho_{S_{n_{0k}}S_{PIE_{1k}}} \\ \rho_{N_{0k}S_{PIE_{0k}}} & \rho_{S_{0k}S_{PIE_{0k}}} & \rho_{S_{n_{0k}}S_{PIE_{0k}}} & 1 & \rho_{S_{PIE_{0k}}N_{1k}} & \rho_{S_{PIE_{0k}}S_{1k}} & \rho_{S_{PIE_{0k}}S_{n_{1k}}} & \rho_{S_{PIE_{0k}}S_{PIE_{1k}}} \\ \rho_{N_{0k}N_{1k}} & \rho_{S_{0k}N_{1k}} & \rho_{S_{n_{0k}}N_{1k}} & \rho_{S_{PIE_{0k}}N_{1k}} & 1 & \rho_{N_{1k}S_{1k}} & \rho_{N_{1k}S_{n_{1k}}} & \rho_{N_{1k}S_{PIE_{1k}}} \\ \rho_{N_{0k}S_{1k}} & \rho_{S_{0k}S_{1k}} & \rho_{S_{n_{0k}}S_{1k}} & \rho_{S_{PIE_{0k}}S_{1k}} & \rho_{N_{1k}S_{1k}} & 1 & \rho_{S_{1k}S_{n_{1k}}} & \rho_{S_{1k}S_{PIE_{1k}}} \\ \rho_{N_{0k}S_{n_{1k}}} & \rho_{S_{0k}S_{n_{1k}}} & \rho_{S_{n_{0k}}S_{n_{1k}}} & \rho_{S_{PIE_{0k}}S_{n_{1k}}} & \rho_{N_{1k}S_{n_{1k}}} & \rho_{S_{1k}S_{n_{1k}}} & 1 & \rho_{S_{n_{1k}}S_{PIE_{1k}}} \\ \rho_{N_{0k}S_{PIE_{1k}}} & \rho_{S_{0k}S_{PIE_{1k}}} & \rho_{S_{n_{0k}}S_{PIE_{1i}}} & \rho_{S_{PIE_{0k}}S_{PIE_{1k}}} & \rho_{N_{1k}S_{PIE_{1k}}} & \rho_{S_{1k}S_{PIE_{1k}}} & \rho_{S_{n_{1k}}S_{PIE_{1k}}} & 1 \end{bmatrix},$$

$$\beta_0^N, \beta_1^N \sim student(3, 5, 10),$$

$$\beta_0^S, \beta_1^S \sim student(3, 3, 10),$$

$$\beta_0^{S_n}, \beta_0^{S_{PIE}}, \beta_1^{S_n}, \beta_1^{S_{PIE}} \sim student(3, 2, 10),$$

$$\sigma^N, \sigma^{S_n}, \sigma^{S_{PIE}}, \sigma_{0i}^S, \sigma_{0j}^N, \sigma_{0j}^S, \sigma_{0j}^{S_n}, \sigma_{0j}^{S_{PIE}}, \sigma_{0k}^N, \sigma_{0k}^S, \sigma_{0k}^{S_n}, \sigma_{0k}^{S_{PIE}}, \sigma_{1k}^N, \sigma_{1k}^S, \sigma_{1k}^{S_n}, \sigma_{1k}^{S_{PIE}} \sim student(3, 0, 10),$$

$$\boldsymbol{R} \sim LJK(1),$$

where N_{ijk}, S_{ijk}, $S_{n_{ijk}}$, and $S_{PIE_{ijk}}$ are the values of each of the metrics for the *i*th concatenation of source ID, study number, block and site number (denoted SSBS in the database), in the *j*th concatenation of source ID, study number, block (denoted SSB in the database), of the *k*th combination of source ID and study (denoted SS in the database), and *LU* is an identifier for land use types (other than primary vegetation, that was fit as the intercept). β_0 (with the respective superscripts for each metric) represent the non-varying intercepts for reference land use category (i.e., primary vegetation). β_{0i}^{S} is a site-level varying intercept to model overdispersion in *S*. β_{0j} (with the respective superscripts for each metric) is a varying intercept for blocks. β_{0k} and β_{1k} (with the respective superscripts for each metric) represent the varying intercepts (reference sites for each study) and slopes (departures for all other sites). The covariance matrix of the multivariate normal distribution for varying study-site effects were parameterised in terms of a correlation matrix **R** and two matrices **S** with diagonal elements σ (superscripts for metrics, subscripts denote intercept (0), slopes (1)).

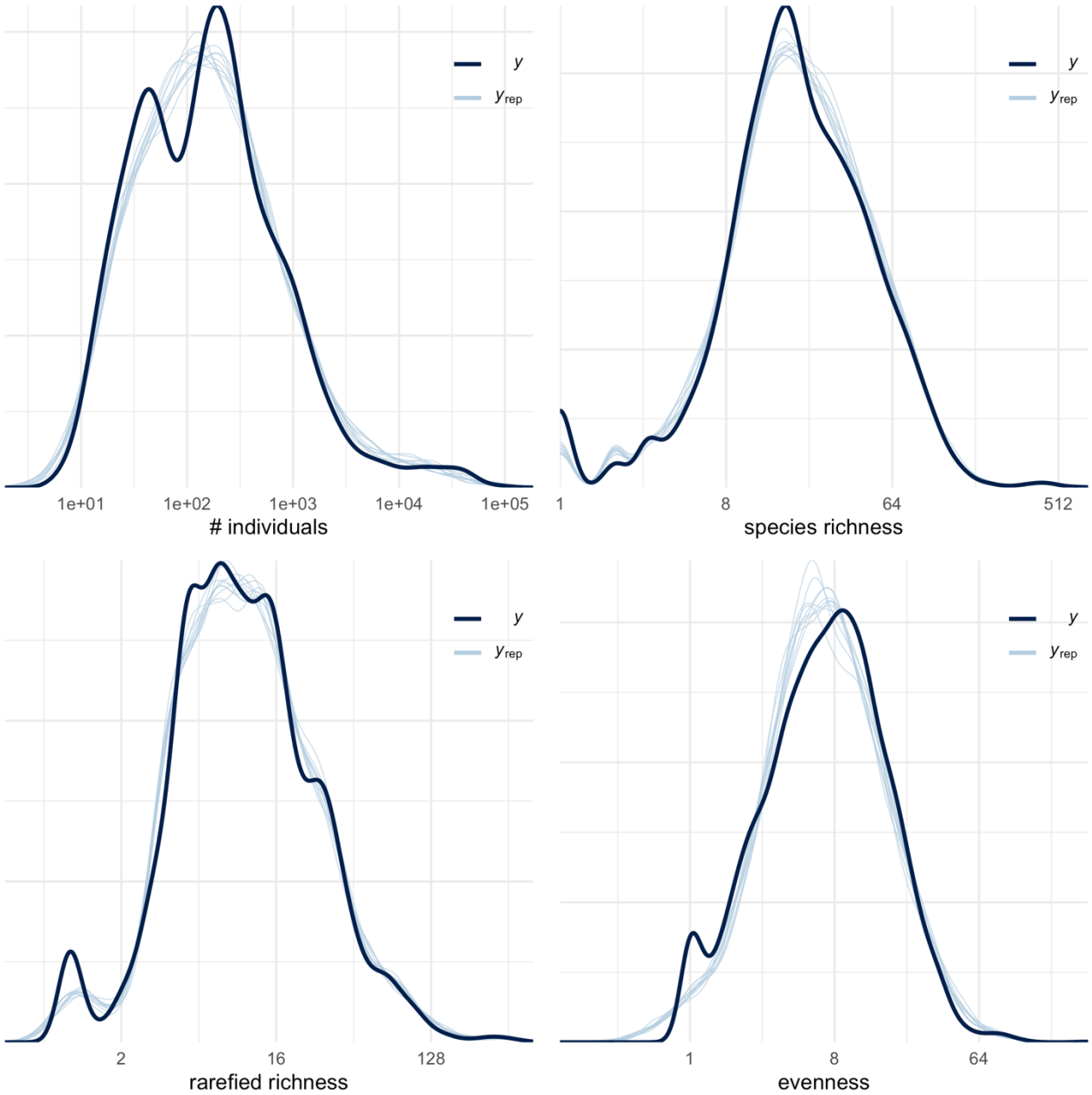

Figure S4: Posterior predictive checks for the model fit to the spatial data in anthropogenically perturbed environments. (a) Total numbers of individuals, (b) species richness, (c) rarefied richness (S_n) and (d) evenness (S_{PIE}). Each panel shows the density of the data (y) and ten draws of the posterior distribution (yrep).

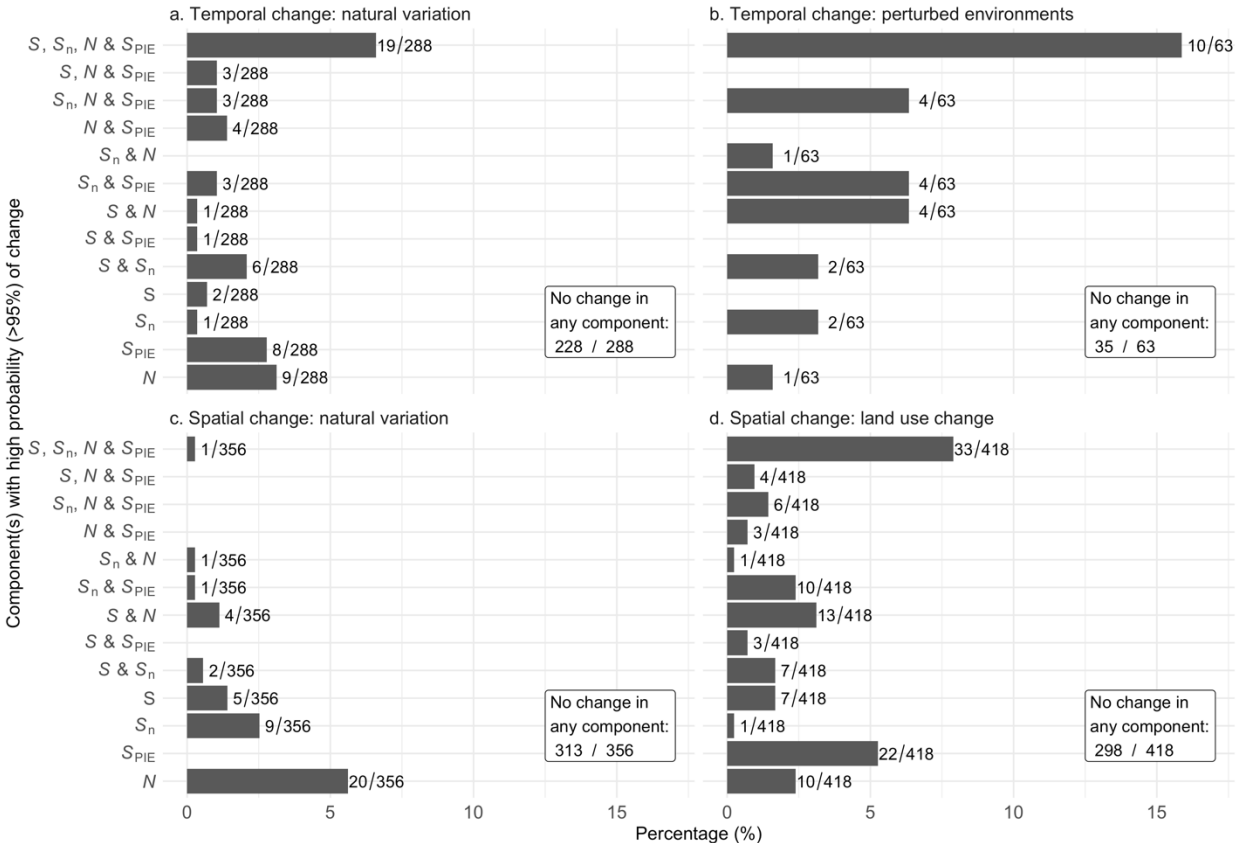

Figure S5: Summary of assemblage diversity components with a high probability of change (90% credible interval did not overlap zero).(a) temporal changes in naturally varying environments, (b) temporal changes in perturbed environments, (c) spatial changes relative to an arbitrary reference, (d) spatial changes relative to primary vegetation. Assemblages with no component changes different from zero are reported as insets for clarity. Metric abbreviations: total number of individuals (N), expected number of species for n individuals (S_n), numbers equivalent transformation of the Probability of Interspecific Encounter (S_{PIE}), and total species richness (S). Number following each bar is the count of assemblages for that category.

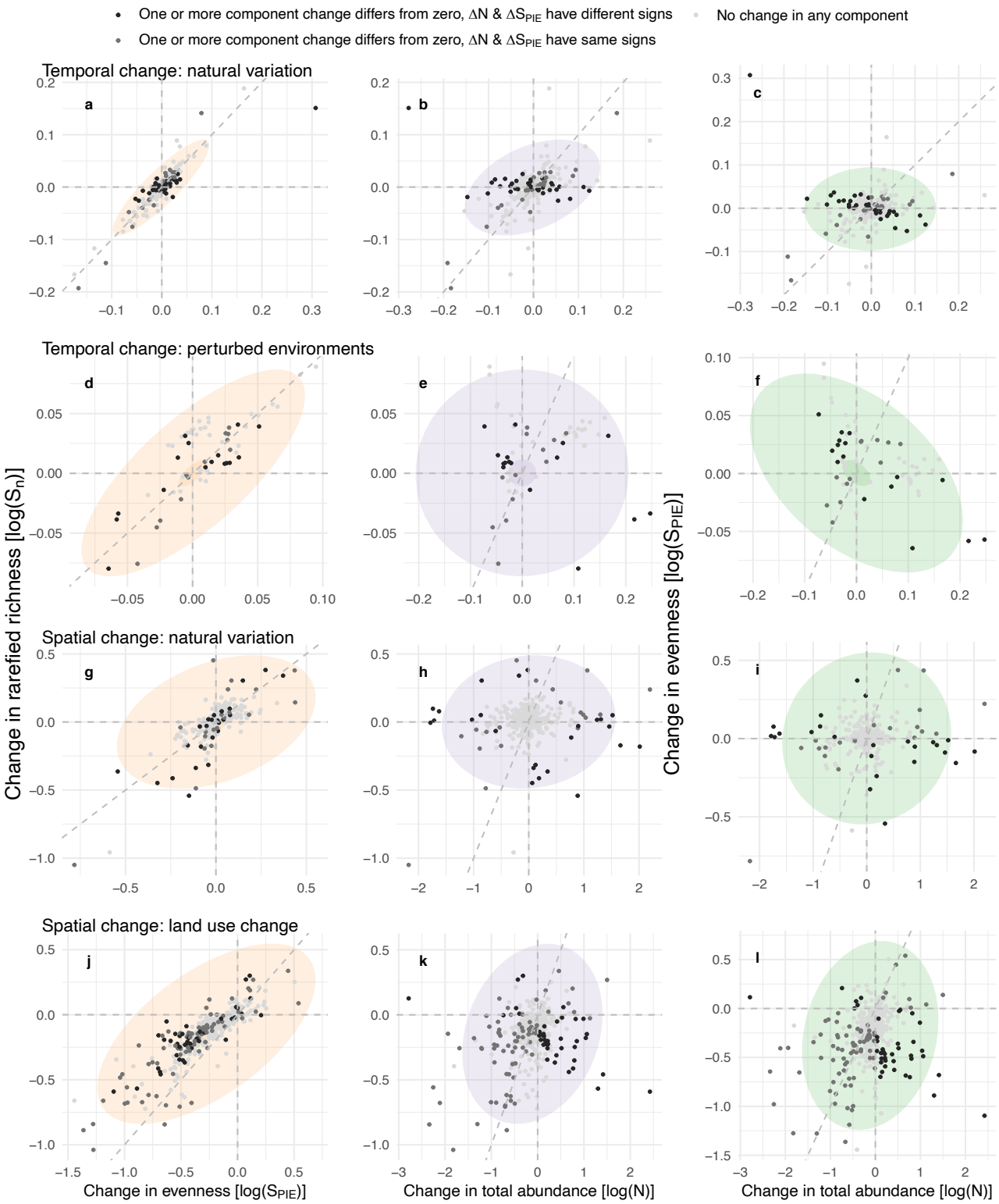

Figure S6: Relationships between four components of local diversity change (not shown on Figure 3). Change in rarefied richness as a function of changes in evenness (left), change in rarefied richness as a function of changes in total abundance (middle) and evenness (right) for (a-c) study-level estimates of temporal changes in naturally varying environments; (d-f) estimates of temporal change for combinations of study and treatment in perturbed environments; (c) estimates of spatial changes within studies from an arbitrary reference site along natural

environmental gradients; and, (d) estimates of spatial change within studies between primary vegetation and different land use categories. Coloured concentration ellipses show 10% increments (5 – 95%) of the posterior distributions. Dotted grey lines are x = y = 0, and x = y for visual reference. NB: Scale of x- and y-axes vary between data sources; one estimate with ΔN = -1.79, ΔS = -3.77, ΔSn = -3.23, ΔSPIE = -3.21, removed from (j-l) for clarity.